Shifts in the rhizobiome during consecutive *in planta* enrichment for phosphate-solubilizing bacteria differentially affect maize P status

Noémie De Zutter[1,2,*] iD Maarten Ameye,[1] iD
Jane Debode,[3] iD Caroline De Tender,[3,4] iD
Sarah Ommeslag,[3] iD Jan Verwaeren,[5] iD
Pieter Vermeir,[6] iD Kris Audenaert[1,†] iD and
Leen De Gelder[2,†] iD

[1]*Laboratory of Applied Mycology and Phenomics (LAMP), Department of Plants and Crops, Faculty of Bioscience Engineering, Ghent University, Valentin Vaerwyckweg 1, Ghent, B-9000, Belgium.*
[2]*Laboratory of Environmental Biotechnology, Department of Biotechnology, Faculty of Bioscience Engineering, Ghent University, Valentin Vaerwyckweg 1, Ghent, B-9000, Belgium.*
[3]*Plant Sciences Unit, Flanders Research Institute for Agriculture, Fisheries and Food (ILVO), Burgemeester Van Gansberghelaan 96, Merelbeke, B-9820, Belgium.*
[4]*Department of Applied Mathematics, Computer Science and Statistics, Ghent University, Krijgslaan 281 S9, Ghent, B-9000, Belgium.*
[5]*Research Unit Knowledge-based Systems (KERMIT), Department of Data Analysis and Mathematical Modeling, Ghent University, Coupure links 653, Ghent, B-9000, Belgium.*
[6]*Laboratory of Chemical Analysis (LCA), Faculty of Bioscience Engineering, Ghent University, Valentin Vaerwyckweg 1, Ghent, B-9000, Belgium.*

Summary

Phosphorus (P) is despite its omnipresence in soils often unavailable for plants. Rhizobacteria able to solubilize P are therefore crucial to avoid P deficiency. Selection for phosphate-solubilizing bacteria (PSB) is frequently done *in vitro*; however, rhizosphere competence is herein overlooked. Therefore, we developed an *in planta* enrichment concept enabling simultaneous microbial selection for P-solubilization and rhizosphere competence. We used an ecologically relevant combination of iron- and aluminium phosphate to select for PSB in maize (*Zea mays* L.). In each consecutive enrichment, plant roots were inoculated with rhizobacterial suspensions from plants that had grown in substrate with insoluble P. To assess the plants' P statuses, nondestructive multispectral imaging was used for quantifying anthocyanins, a proxy for maize's P status. After the third consecutive enrichment, plants supplied with insoluble P and inoculated with rhizobacterial suspensions showed a P status similar to plants supplied with soluble P. A parallel metabarcoding approach uncovered that the improved P status in the third enrichment coincided with a shift in the rhizobiome towards bacteria with plant growth-promoting and P-solubilizing capacities. Finally, further consecutive enrichment led to a functional relapse hallmarked by plants with a low P status and a second shift in the rhizobiome at the level of Azospirillaceae and Rhizobiaceae.

Introduction

Plants live in close association with soil microbes present in their rhizosphere through cross-kingdom communication, which is based on mutual signalling mechanisms (Spaepen *et al.*, 2007; Oldroyd, 2013; Kai *et al.*, 2016; Schirawski and Perlin, 2018). Through root exudates, bacteria from bulk soil are actively recruited by the plant into its rhizosphere. One of the most important groups of beneficial rhizosphere microbiota is plant growth-promoting rhizobacteria (PGPR), which are able to colonize the rhizosphere and stimulate plant growth (Khan *et al.*, 2007; Robin *et al.*, 2008; Raaijmakers *et al.*, 2009; Smercina *et al.*, 2019).

Phosphorus (P) is one of the limiting macronutrients in plant growth as most of the total P is either bound to recalcitrant organophosphates or fixed with metals, both which must be mineralized to phosphate (Pi) before it can be assimilated by plants (Raghothama, 2000). Microbial phosphate solubilization is therefore an important biostimulatory trait considering the eutrophic effects of runoff by excessive chemical P fertilizers and the declining phosphorus stocks worldwide (Cordell *et al.*, 2009; Bhattacharyya and Jha, 2012; Reijnders, 2014). P-solubilizing bacteria (PSB) are able to solubilize

phosphate through different mechanisms, such as the production of enzymes (phytase and phosphatase), organic acids and siderophores (Khan *et al.*, 2009; Sharma *et al.*, 2013; Pii *et al.*, 2015; Neal *et al.*, 2018; Udaondo *et al.*, 2020).

PSB, and more generally PGPR, are being hailed as a source of promising biostimulants for agri- and horticulture (Compant *et al.*, 2010). However, as stated by Toju et al. (2018), commercialized PGPR introduced to farmlands often rapidly decline or do not fulfil the ecological task for which they were initially introduced. This is partially due to the most adopted screening techniques being the *in vitro* screening for P-solubilizing traits on microbiological media (Nautiyal, 1999; Mehta and Nautiyal, 2001; Liu *et al.*, 2016). Isolates that looked promising in the laboratory often fail to deliver in pot or field trials (Chauhan *et al.*, 2015). The major factors that adversely affect bacterial efficiency in the field are (i) the soil physicochemical properties of farmlands, which differ largely from laboratory trials; (ii) the bacterial inability to colonize the plant rhizosphere, resulting in the lack of so-called rhizosphere competence (Bach *et al.*, 2016; Amaya-Gómez *et al.*, 2020); (iii) and the strict mutual dependencies and competition in the rhizobiome (Benizri *et al.*, 2001; Schink, 2002; Barea *et al.*, 2005; Babalola, 2010; de Souza *et al.*, 2015; Backer *et al.*, 2018). The rationale behind this current study is that the rhizosphere environment is not included in the *in vitro* screenings for PSB, while the plant–bacteria interactions are paramount in securing effective plant growth-promoting traits (Schloss and Handelsman, 2005; Bais *et al.*, 2006; Lebeis *et al.*, 2012; Stewart, 2012; Castrillo *et al.*, 2017). The rhizosphere is a highly dynamic environment in which specific root exudates can cause distinct shifts in bacterial communities (Bais *et al.*, 2006; Lynch and de Leij, 2001; Dakora and Phillips, 2002; Li *et al.*, 2019). Such shifts have already been described in the rhizosphere of plants under iron deficiency (Yang and Crowley, 2000) and nitrogen and phosphorus deficiency (Wasaki *et al.*, 2018). Metagenome studies indicate that Proteobacteria, Actinobacteria and Bacteroidetes are amongst the most dominant phyla in the rhizosphere. Belonging to those phyla, *Azospirillum*, *Burkholderia*, *Pseudomonas*, *Rhizobium* and *Enterobacter* are described as highly efficient PSB described in literature (Sigurbjörnsdóttir *et al.*, 2015; Li *et al.*, 2019).

Few studies are available in which active selection on the ability of rhizosphere colonization is incorporated in an enrichment strategy (Kuiper *et al.*, 2001; Kamilova *et al.*, 2005). In Kuiper et al. (2001), a new polycyclic hydrocarbon-degrading strain was isolated from the enrichment culture which colonized the root tip up to 100-fold more than the PGPR *Pseudomonas fluorescens* WCS365. Another study (Etesami *et al.*, 2014)

incorporated interactions of isolates, previously obtained by plating on Tryptic Soy Agar with the root system in order to re-isolate plant growth-promoting endophytic bacteria. All re-isolated strains were consistently more active in colonizing seedlings. Wang et al. (2021) performed an *in vitro* screening for PGPR on selective medium in which root exudates were used as a sole carbon source as an alternative method to select for rhizosphere competent microorganisms. Finally, community-based culture collections (CBC) are a new strategy for selecting microbial isolates or consortia with a high potential to colonize different plant parts. This strategy comprises a large-scale isolation of plant-associated organisms. These plant-associated microbial communities are annotated, and synthetic communities are assembled based on naturally occurring highly abundant bacterial groups (Armanhi *et al.*, 2018). The synthetic communities can then be used as artificial plant inocula to colonize plant roots.

To resolve the need for the selection of rhizosphere competent bacteria, we developed and validated a consecutive *in planta* enrichment platform to enrich the maize rhizosphere for PSB in the presence of iron and aluminium phosphates as insoluble P sources. These are amongst the main P sources present in the slightly acidic European soils (Reuter *et al.*, 2008; Amery and Vandecasteele, 2015) and therefore a more ecologically relevant choice for PSB selection compared to the most commonly used tri-calcium phosphate (Bashan *et al.*, 2013). Several consecutive *in planta* enrichments were carried out, in which the rhizosphere suspensions obtained in the previous *in planta* trial were used as inoculum for the subsequent trial. The maize plants were monitored throughout each consecutive trial using an automated multispectral camera, measuring the modified anthocyanin reflectance index (mARI) as a proxy for the P status of the maize plants. Anthocyanin accumulation is commonly used as a proxy for P deficiency, and a relationship between the anthocyanin content and P deficiency has been established for several plants (Ulrychová and Sosnová, 1970; Stewart *et al.*, 2001; Osborne *et al.*, 2002; Jiang *et al.*, 2007; Yaryura *et al.*, 2009; Li *et al.*, 2014; Wang *et al.*, 2018b). Furthermore, changes in the rhizosphere population during the consecutive enrichments were monitored using bacterial 16S amplicon sequencing. In this study, we showed how a consecutive *in planta* enrichment approach differentially affects the maize P status and can lead to the selection of an efficient P-solubilizing consortium.

Results

Establishing the link between anthocyanins, mARI and P content

The correlation between mARI and anthocyanin content was evaluated in a separate trial with plants grown

under different P concentrations. A significant linear regression (Eq. 1) was calculated to predict anthocyanin content based on mARI (Fig. 1A) ($F(1,47) = 51.683$, $P < 0.001$) with an R^2 of 0.524.

$$Anthocyanin\,content = 16.02 + 96.38\,(mARI)\,mgl^{-1}. \quad (1)$$

To determine whether the mARI is an appropriate indicator of maize P content, the relationship between mARI and P content was assessed (Fig. 1B). The relationship between mARI and P content can be described by the following exponential (least-squares regression) model: $mARI = 0.623 + 7.14e^{-0.00152P} (R^2 = 0.809)$, where P is the observed P content. This relationship in maize is comparable to the earlier described exponential model for tobacco (Li *et al.*, 2014). To fully comprehend this relationship, three biologically relevant thresholds were defined: one at 2000 mg P per kg dried plant material, based on the approximated biologically minimum P content present in P-deficient maize plants due to the P-reserves in the kernel (Gwirtz and Garcia-Casal, 2014; Guo *et al.*, 2018); a second threshold at 5000 mg P per kg dried plant material, based on the expected P content of young, healthy maize plants (Plank, 1989); and a third threshold at mARI 0.623, based on the tail of the exponential distribution. Plants with a P content below 5000 mg P.(kg DW)$^{-1}$ cover a range of mARI values

from 0-5, while plants with a P content above 5000 mg P.(kg DW)$^{-1}$ stabilize around an mARI value of 0.623.

Assessment of the *in planta* enrichment platform

In vitro parameters. The rhizosphere start suspension (RSS) and the enriched rhizosphere suspensions obtained from the validation experiment (V-B1, B2, B3 and B4; Fig. 2A) were plated on LB agar and MPVK agar with iron and aluminium phosphate as insoluble P sources and evaluated for their P-solubilizing capacity in liquid NBRIP medium (Table 1). On both LB and MPVK agar, bacterial counts of the enriched suspensions were significantly higher than bacterial counts of the RSS (one-way ANOVA; $F(4,22) = 12.380$, $P < 0.001$ resp. $F(4,22) = 20.198$, $P < 0.001$) but no differences were observed between the enriched suspensions. There were no significant differences between the enriched suspensions in the qualitative evaluation of organic acid production on MPVK agar. Finally, the P-solubilizing capacities of the RSS and enriched suspensions were quantitatively assessed. RSS, V-B3 and V-B4 were able to solubilize significantly more phosphate than the uninoculated, sterile blanc (two-sample t-test, $t(3) = 5.276$, $P = 0.013$; $t(7) = 7.343$, $P < 0.001$; resp. $t(7) = 2.888$, $P = 0.023$), but no differences were found between the enriched suspensions and the RSS. In
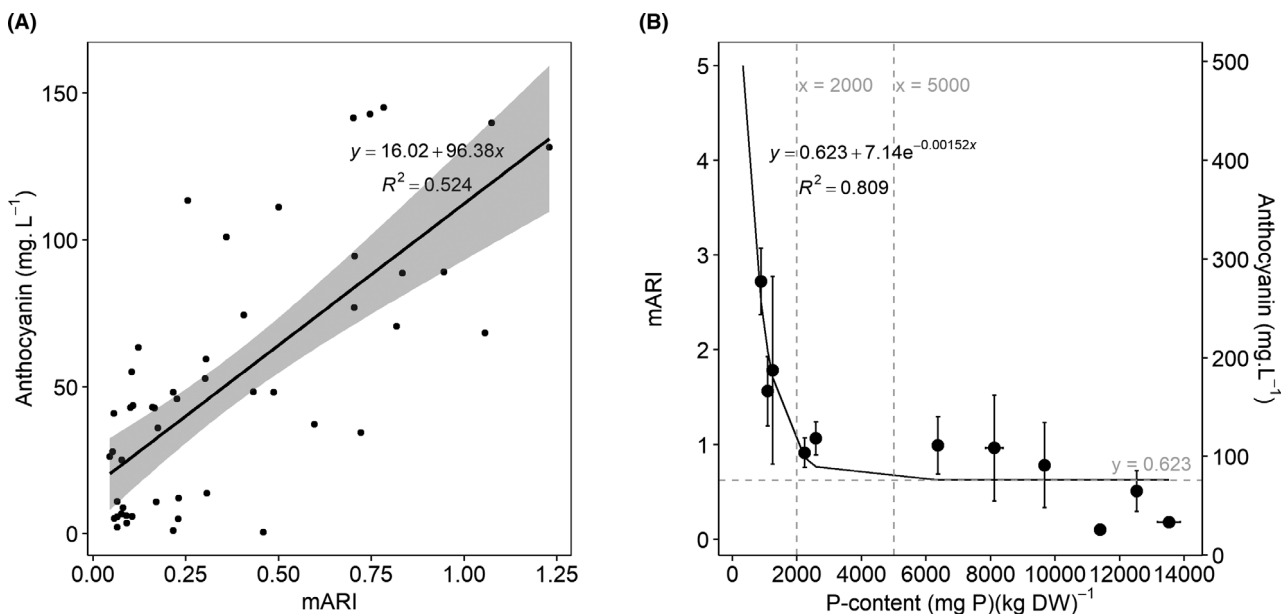

Fig. 1. A. Linear regression model to link the modified anthocyanin reflectance index (mARI) to anthocyanin content in maize plants. Grey shadow represents the 95% confidence interval around the slope of the regression line.
B. Exponential relationship between the modified anthocyanin reflectance index (mARI) and P content in maize. Values (•) represent mean ± se of different P groups; exponential regression established through least square regression. Lower limits of P content for actively growing maize plants (5000 mg P per kg dried plant material) and the residual P content in maize plants due to the P reserves in the seed (2000 mg P per kg dried plant material) are indicated with a dashed line, as well as the mARI threshold (0.6) determined by the tail of the exponential curve.
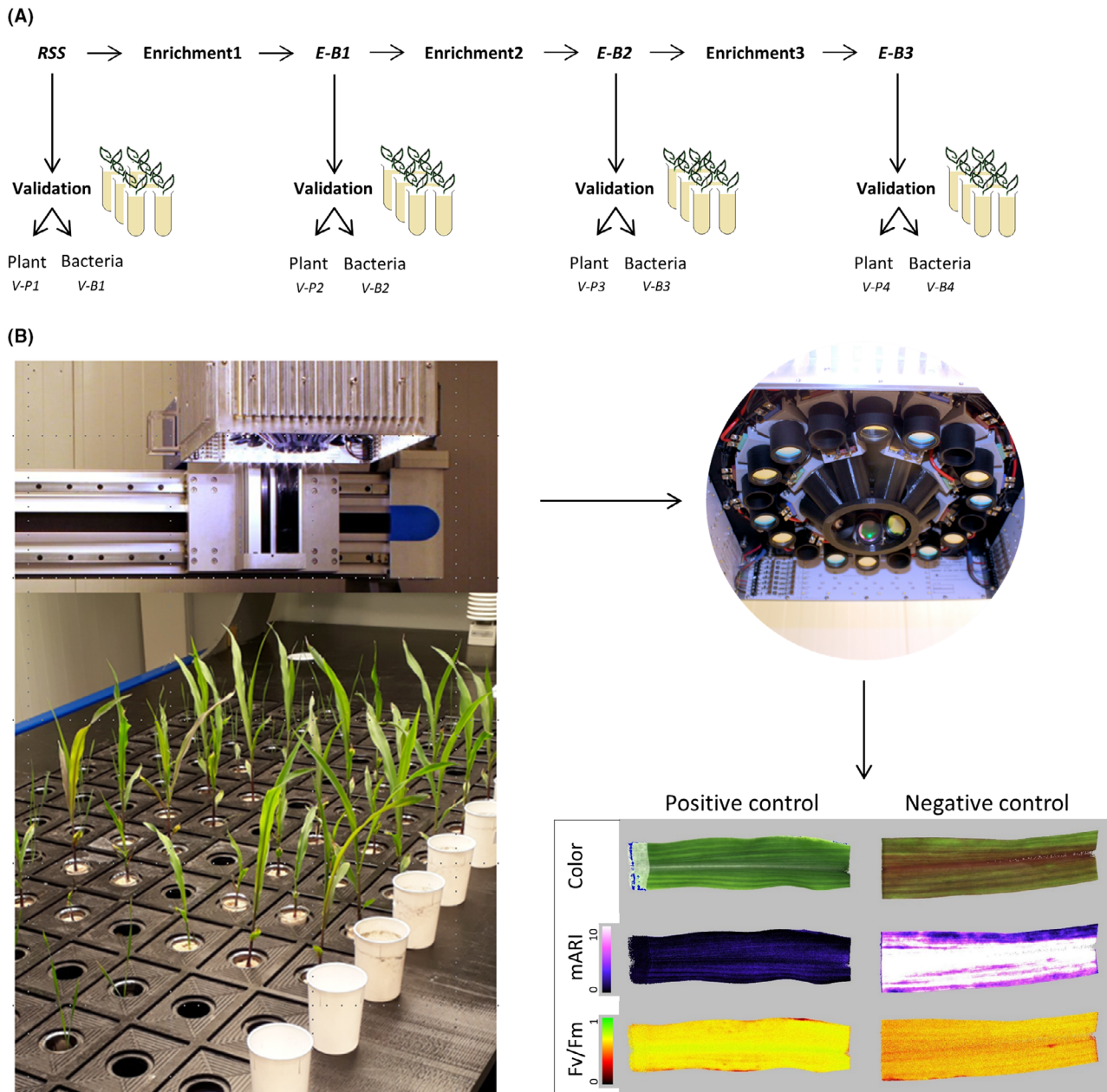
(A)

(B)

Fig. 2. A. Experimental design of enrichments *(E)*, enriched cultures and plant and bacterial material obtained in a validation experiment *(V)*. *RSS*: Rhizosphere start suspension; *Bn*: bacterial suspension isolated from enrichment *n*.
B. Overview of the *in planta* validation experiment housed in an acclimatized growth chamber, provided with a camera for multispectral imaging. Detailed colour image and false colour image of anthocyanin (mARI) and chlorophyll fluorescence (Fv/Fm) of detached leaves of a positive control (supplied with soluble P) and a negative control (supplied with insoluble P).

conclusion, this *in vitro* approach gave some indications for the presence of PSB in the enriched suspensions (e.g. growth on selective medium); however, no indications of functional nor numeric differences between the enriched suspensions.

Plant growth-promoting traits. Both the rhizosphere start suspension and the enriched suspensions were assessed for plant growth-promoting traits in an overall *in planta* validation trial coupled to a multispectral imaging platform (Fig. 2B). An overview of the plants at the end of the experiment can be found in Fig. S1. As P-solubilization is often linked to plant growth promotion, shoot length and shoot dry weight were determined (Table 2). Plant length and dry weight were not significantly affected by inoculation with enriched

Table 1. *In vitro* phosphate parameters: growth on rich (LB) and selective (MPVK) media, P-solubilization in liquid medium (NBRIP-*FeP:AlP*) and production of organic acids (MPVK).

Treatment*	LOG(CFU) per gram roots		Dissolved P (mg P l^{-1})**	Production of organic acids (%)
	LB	MPVK		
RSS	6.6 ± 0^a	6.0 ± 0.4^a	$42.0 \pm 2.0^{(*)}$	6.4 ± 1.8^a
V-B1	7.9 ± 0.4^b	8.2 ± 0.5^b	33.2 ± 9.2	10.6 ± 6.9^a
V-B2	8.4 ± 0.5^b	8.4 ± 0.4^b	52.2 ± 26.6	10.7 ± 5.6^a
V-B3	7.8 ± 0.2^b	8.1 ± 0.5^b	$43.9 \pm 4.1^{(*)}$	7.6 ± 6.0^a
V-B4	7.9 ± 0.4^b	8.5 ± 0.3^b	$49.1 \pm 14.0^{(*)}$	5.3 ± 3.4^a
Sterile blanc	–	–	24.8 ± 3.3	–

Values represent the means of six (V-Bn) or three (RSS) biological replicates $\pm$ SD. (a–b) Data with the same letter in superscripts per column are not significantly different at 5% probability level as per ANOVA and a *post hoc* Tukey test or Dunnett-T3 test.
*. RSS: Rhizosphere start suspension; V-B1-4: Enriched bacterial cultures isolated after the validation experiment (Fig. 2A).
**. Significant differences from sterile blanc at 5% probability level indicated $^{(*)}$ as per two-sample *t*-test.

Table 2. *In planta* parameters of maize (*Zea mays* L.) after 21 days growth: length (cm), shoot dry weight (mg) and efficiency of photosystem II (Fv/Fm value).

Treatment*	Length (cm)	Shoot dry weight (mg)	Fv/Fm
Positive control	36.1 ± 12.2	390 ± 170	0.647 ± 0.028^a
Negative control	45.0 ± 8.5	580 ± 246	0.519 ± 0.081^b
V-P1	41.9 ± 7.0	511 ± 155	0.586 ± 0.076^{ab}
V-P2	41.2 ± 15.5	533 ± 265	0.557 ± 0.060^{ab}
V-P3	28.9 ± 12.3	300 ± 226	0.603 ± 0.045^{ab}
V-P4	42.3 ± 3.8	530 ± 157	0.635 ± 0.022^a

Values represent the mean of six biological replicates $\pm$ SD. (a–b) Data with the same letter in superscripts per column are not significantly different at 5% probability level as per ANOVA and a *post hoc* Tukey test. If none of the treatments differed significantly, no indications were made.
*. Positive control: uninoculated plants supplied with soluble P (KH$_2$PO$_4$); Negative control: uninoculated plants supplied with insoluble P (FeP:AlP); V-Pn: inoculated with bacterial suspensions, plants supplied with insoluble P (FeP:AlP) (Fig. 2A).

suspensions, nor by the presence of a soluble P source (positive control) (one-way ANOVA, $F_{(5,30)} = 1.794$, $P = 0.144$; resp. $F_{(5,30)} = 1.569$, $P = 0.199$). Counterintuitively, the average shoot length of the positive control plants was lower than the negative control plants. This effect can be ascribed to the prevalence of twisted and tightly folded, sticky whorls (Fig. S2A). V-P2-4 plants were similarly affected compared to the positive control plants (Pearson chi-square test; $P = 0.221$, resp. $P = 0.505$, resp. $P = 0.221$), while V-P1 and negative control plants showed a significant lower prevalence of twisted whorls ($P = 0.021$ for both) (Fig. S2B). Additionally, the efficiency of photosystem II (PSII, Fv/Fm value) was determined. The highest Fv/Fm values were observed in the positive control, V-P3 and V-P4 (Table 2).

mARI and nutrient content. Under the chosen growth conditions, the detection of anthocyanin accumulation through the mARI became apparent at day 18 (Fig. 3A) after which it rapidly increased and a visible purple discoloration manifested. Destructive end-point mARIs were compared to the non-destructive measurements at several time points (data not shown) and were found to be significantly positive correlated from day 19 onwards ($P < 0.001$).

Pixels from images of the detached leaves were divided into two classes based on their mARI value (class I: mARI<0.6; class II: mARI>0.6) (Fig. 3B; Fig. S3). Classes were based on the exponential fit between mARI and P content (Fig. 1) and were in accordance with the 95% confidence interval of the positive control plants (Fig. S4). The negative control had a significantly lower proportion of pixels in class I compared to the positive control (two-sample t-test, $t(10) = 3.277$, $P = 0.011$), indicating a clear P deficiency which is expected from the negative control. Similarly, V-P1 and V-P2 also had a significant lower proportion of pixels in class I compared to the positive control ($t(10) = 2.007$, $P = 0.037$; resp. $t(10) = 3.518$, $P = 0.008$), indicating the P deficiency was not (fully) relieved by adding these bacterial suspensions. In V-P3 and V-P4, the number of pixels in class I was similar to the positive control ($t(10) = 0.733$, $P = 0.241$; resp. $t(10) = 1.023$, $P = 0.167$). This indicated that after two enrichments, plant stress levels due to P deficiency were reduced due to the enriched suspensions.

It is expected that the P content of young, actively growing, healthy plants exceeds 0.5%, which corresponds to 5000 mg P per kg dried plant material. As an excess of P was administered, positive control plants contained significantly more phosphorus than 5000 mg P.kg^{-1} (one-sample t-test, $t(6) = 10.292$, $P < 0.001$) (Fig. 3C), while the negative control, V-P1 and V-P4 contained significantly less P than 5000 mg P.kg^{-1} ($t(5) = -14.305$, $P < 0.001$; resp. $t(6) = -7.701$, $P = 0.001$; resp. $t(6) = -5.539$, $P = 0.003$). V-P2 and V-P3 showed no significant differences from 5000 mg P.kg^{-1} ($t(6) = -1.594$, $P = 0.172$; resp. $t(6) = 0.528$, $P = 0.620$). A partial uncoupling of mARI with plant P content in P-deficient circumstances is observed in V-P4, as these plants show low mARI values but also have a low P content (Fig. 3B,C). Finally, the link between mARI and P in the validation experiment followed the expected exponential relationship (Fig. S5).
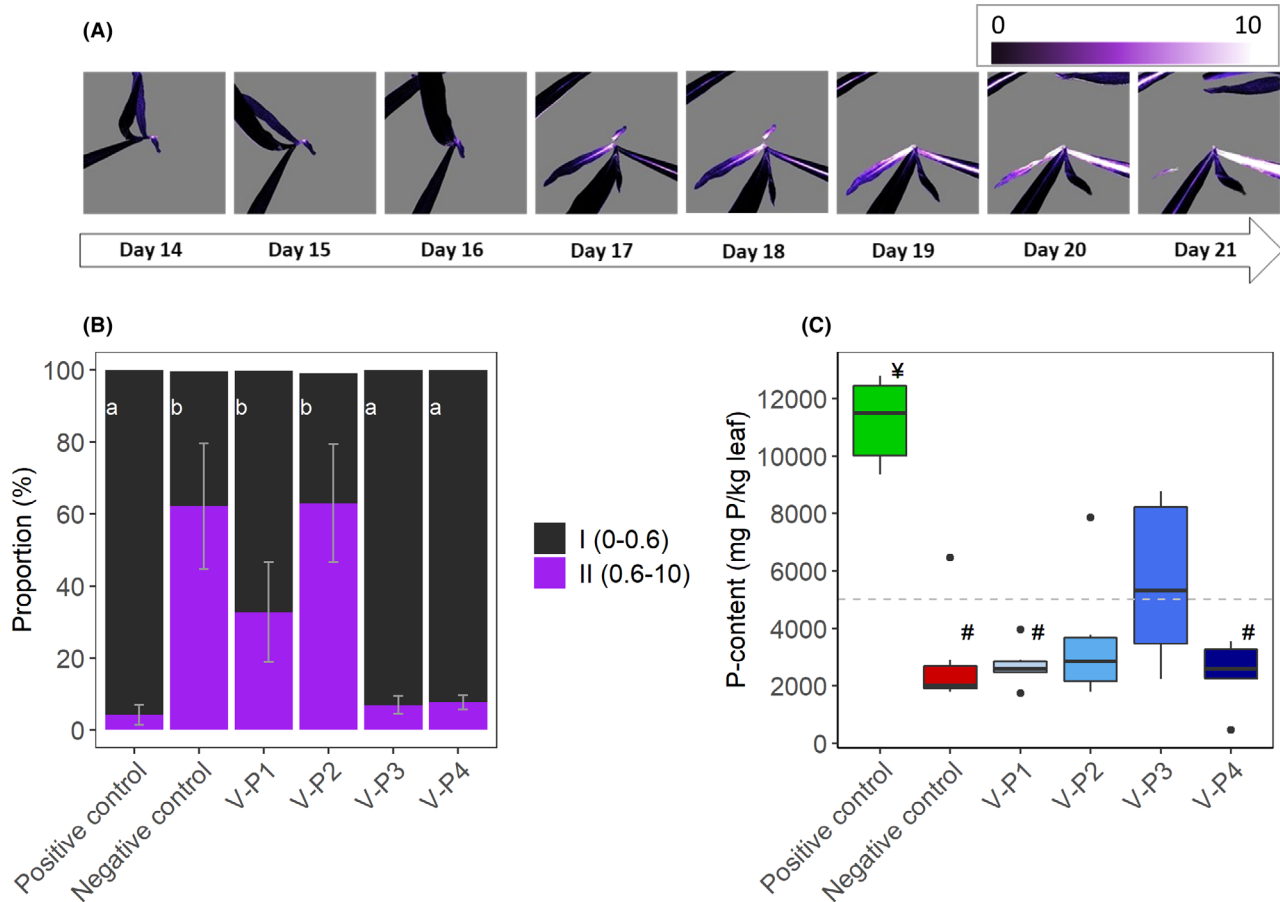
Fig. 3. A. False colour image of a maize plant (top view) in time, indicating the emerging of anthocyanin accumulation from day 17 onwards. Dark pixels represent low mARI values (low anthocyanin content), purple to white pixels represent high mARI values (high anthocyanin content).

B. Proportional distribution of leaf pixels in mARI classes. The two mARI classes are based on the 95% confidence interval of plants under full Hoagland solution (= Class I), as these plants are not under P deficiency and therefore showed the optimal phenotype. Error bars denote SD. Significant differences after a two-sample t-test are indicated by letters above the stacked diagrams.

C. Plant P content measured through ICP-OES. Error bars denote S.

D. Mean P contents were compared to a threshold of 5000 mg P per kg dried plant and significant differences as per one-sample *t*-test are indicated with ¥ (P content > 5000) and # (P content < 5000).

Positive control: uninoculated plants supplied with soluble P (KH_2PO_4); Negative control: uninoculated plants supplied with insoluble P (FeP: AlP); *V-Pn*: plants inoculated with RSS (V-P1) or E-B1-3 (V-P2-4), growth substrate supplied with insoluble P (FeP:AlP).

Additionally, the N:P ratio and K:P ratio were assessed in order to evaluate possible pleiotropic effects in the maize plants (Table S1). A constant N:P or K:P ratio implies that N and P uptake is approximately equal, while a decreasing ratio implies that the effect is specifically described to P uptake. In this experiment, the N:P and K:P ratio in the positive control is significantly lower than the N:P and K:P ratio in the treatments (one-way ANOVA and *post hoc* Tukey; $F(5,26) = 10.880$, $P < 0.001$; resp. $F(5,26) = 13.280$, $P < 0.001$), while the ratio remains constant within the different treatments. For the treatments this means that, in plants with a higher P content, N and K uptake are also improved.

Effect of in planta *enrichments on the rhizosphere community*

A total of 6237 unique ASVs were found in the complete, unfiltered data set. After filtering, a total of 1966 unique ASVs were retained. Species richness, diversity and evenness were analysed for the rhizosphere start suspension and enriched suspensions (Table 3). All three indices were significantly higher in the RSS compared to the enriched suspensions (ANOVA, $P < 0.05$). As V-B1 to B4 are enriched suspensions with the RSS as a starting point, these data indicate that a selection occurred during consecutive enrichment. Additionally, we found

Table 3. Species richness (Chao1 index), Shannon diversity and Pielou's evenness.

Treatment*	Chao1 richness	Shannon diversity	Pielou's evenness
RSS	1632 ± 249[a]	6.44 ± 0.05[a]	0.87 ± 0.01[a]
V-B1	231 ± 30[b]	3.52 ± 0.31[b]	0.65 ± 0.04[b]
V-B2	206 ± 20[b]	3.49 ± 0.32[b]	0.66 ± 0.07[b]
V-B3	252 ± 34[b]	3.90 ± 0.23[b]	0.71 ± 0.03[b]
V-B4	228 ± 31[b]	3.45 ± 0.20[b]	0.64 ± 0.02[b]

Values represent the means of six (V-Bn) or three (RSS) biological replicates ± SD. (a–b) Data with the same letter in superscripts per column are not significantly different at 5% probability level as per ANOVA and a *post hoc* Tukey test (diversity and evenness) or Dunnett-T3 test (richness).
*. RSS: Rhizosphere start suspension; V-B1-4: Enriched bacterial cultures isolated after the validation experiment (Fig. 2A).

that the extend of the RSS's richness mainly resulted from low count ASVs, occurring only in the RSS. Finally, based on the median of the enriched suspensions, bacterial evenness is slightly higher in V-B3 compared to the other suspensions, indicating a more even distribution of bacterial species in V-B3.

Beta diversity was assessed by evaluating the bacterial community on different taxonomic levels (phylum, class, order and family). The unfiltered data set contained a total of 31 phyla, 82 classes, 186 orders and 241 families. After filtering the data (minimal abundance of 0.05% in at least six samples), a total of 10 phyla, 13 classes, 33 orders and 45 families were retained. In order of abundance, the Proteobacteria, Bacteroidetes, Firmicutes, Actinobacteria, Cyanobacteria and Verrucomicrobia were the most dominant phyla (Fig. 4A,B). The impact of the consecutive *in planta* enrichment on the original RSS was evaluated to assess which bacterial phyla were enriched or reduced compared to the RSS (Fig. 4A-C). Bacteroidetes, Firmicutes and Cyanobacteria were significantly enriched throughout the enrichments, while other, already low abundant, phyla were even more reduced after enrichment. Metagenome data from the enriched suspensions were coupled to
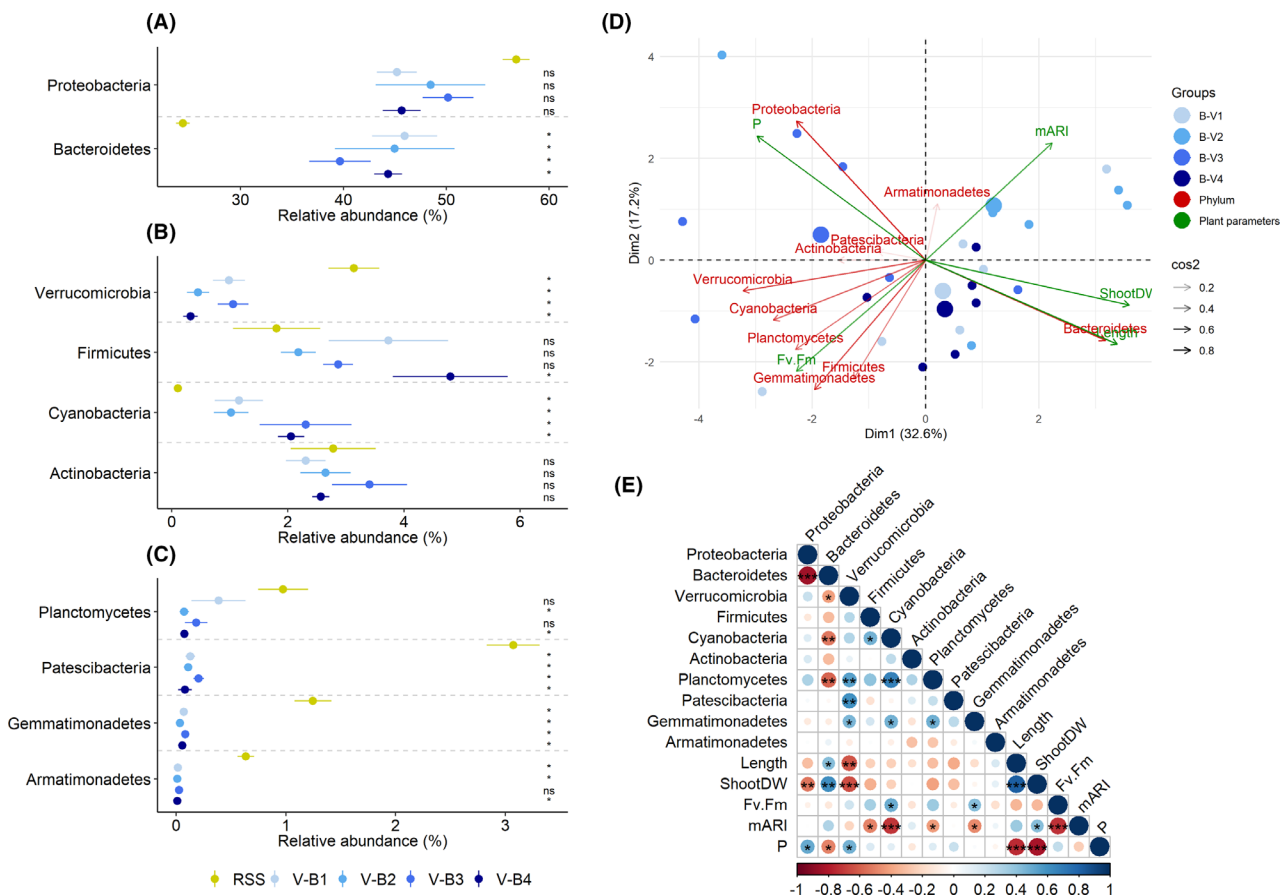

Fig. 4. A–C. Relative abundance of bacterial phyla (resp. high, mid and low abundant phyla) in the rhizosphere start suspension (*RSS*) and enriched suspensions (*V-B1-4*). Values represent the mean of six (*V-B1-4*) or three (*RSS*) biological replicates ± SE.
D. Principal component analysis (PCA) biplot comprising bacterial phyla (red arrows) and plant parameters (green arrows). Samples are coloured according to the corresponding treatment (V-B1 to 4).
E. Spearman correlation matrix between bacterial phyla and important plant parameters

plant parameters obtained in the respective enrichments. Ordination analysis demonstrated that bacterial phyla composition coupled to plant parameters could be explained by the enriched suspensions (Fig. 4D; PER-MANOVA, $R^2 = 0.181$, $P = 0.006$). V-B3 samples are separated from other bacterial suspensions by the first principal component. Finally, when focusing on the enriched suspensions, some phyla were related to the plant parameters P content and mARI. Trends in Proteobacteria and Verrucomicrobia were similar to trends in P content reaching a maximum in V-B3 and relapsing in V-B4, while trends in the abundance of Bacteroidetes were opposite to trends in P content (Figs 3C; 4A, B), both trends that resulted in significant correlations ($P < 0.05$) between these phyla and the plant P contents (Fig. 4E). Another set of phyla, the Firmicutes, Cyanobacteria, Planctomycetes and Gemmatimonadetes followed a course similar to patterns in mARI values (Figs 3B; 4A–C). This trend also resulted in significant correlations between these phyla and mARI (Fig. 4E).

Bacterial phyla that were significantly correlated to either the P status of the plant or the mARI were subsequently evaluated on a lower taxonomic level.

After filtering the data, only 1-3 classes remained within each phylum (Fig. S6A–C). Plant P content was positively correlated with the abundance of Gammaproteobacteria and Verrucomicrobiae, but negatively correlated with the abundance of Bacteroidia in their rhizosphere (Fig. S6D–E). Additionally, mARI was negatively correlated to the Alphaproteobacteria, Bacilli, Oxyphotobacteria, Phycisphaerae and Gemmatimonadetes (Fig. S6E). Finally, the distribution of bacterial orders was evaluated (Fig. S7). As we mainly focus on the enrichment for PSB from the start suspension, we chose to zoom in on the orders that were significantly enriched from the RSS. After applying this additional filter, only five orders were retained (Fig. 5A-C). Ordination analysis for the order-level showed that V-B1 and B2 cluster together, but V-B3 and B4 cluster separately (Fig. 5D; PERMANOVA, $R^2 = 0.193$, $P = 0.028$). The high
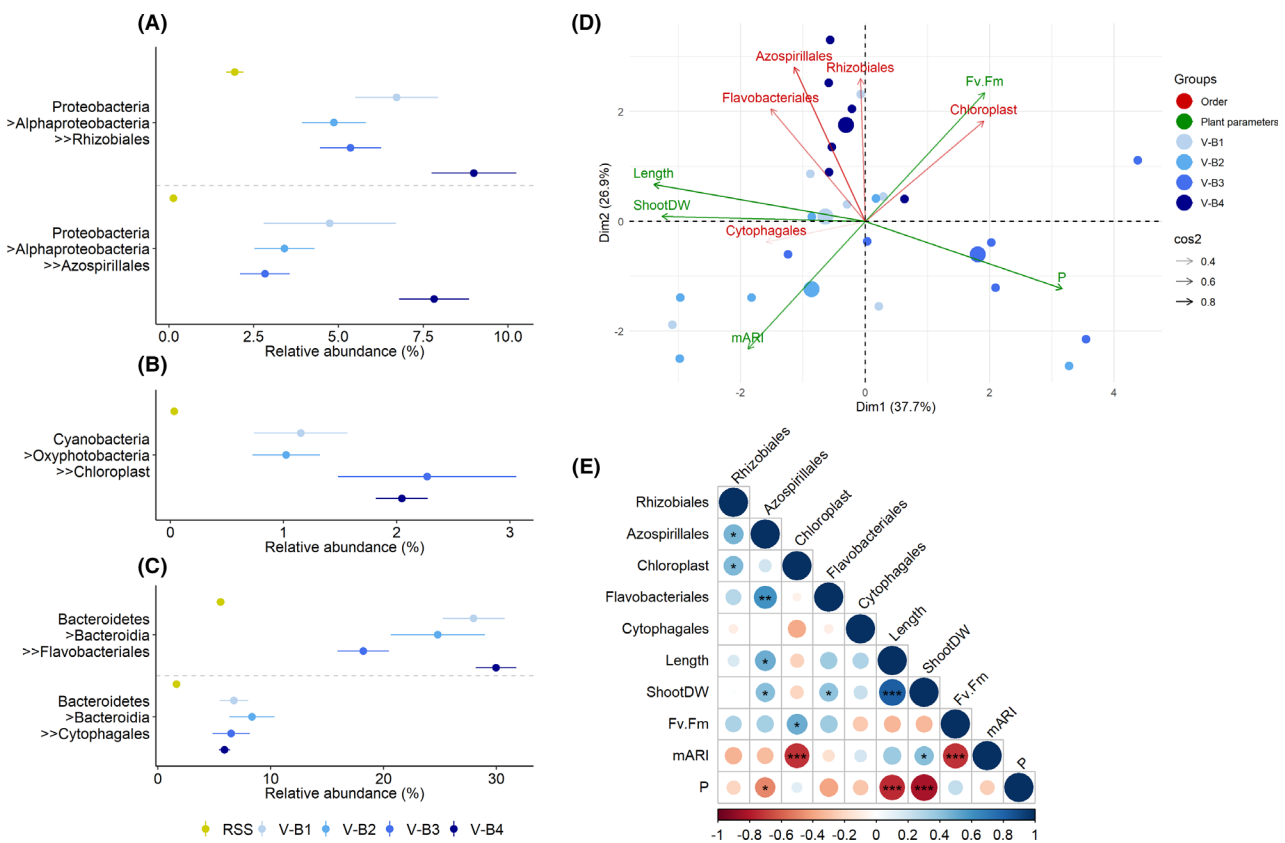

Fig. 5. A-C. Relative abundance of a selection of bacterial orders (resp. belonging to the Gammaproteobacteria, Alphaproteobacteria, Oxyphotobacteria and Bacteroides) in the rhizosphere start suspension (*RSS*) and enriched suspensions (*V-B1-4*). Values represent the mean of six (*V-B1-4*) or three (*RSS*) biological replicates ± SE.
D. Principal component analysis (PCA) biplot comprising bacterial orders (red arrows) and plant parameters (green arrows). Samples are coloured according to the corresponding treatment (V-B1 to 4).
E. Spearman correlation matrix between bacterial orders and important plant parameters.

abundance of Azospirillales, Rhizobiales and Flavobacteriales in V-B4 can be correlated to a lower P content in V-B4 plants (Fig. 5D–E). Belonging to these orders, a significant increase in Azospirillaceae, Rhizobiaceae, Weeksellaceae and Spirosomaceae was observed at family level (Fig. S8).

Discussion

The use of anthocyanin accumulation and its concomitant multispectral derivative, mARI, as a proxy for P deficiency should be considered with care

The accumulation of anthocyanins, which is a part of the flavonoid metabolism in plants, has long been proven a valuable proxy to assess P-starvation in several plant species (Jiang *et al.*, 2007; Wang *et al.*, 2017). Nevertheless, it was only recently that the flavonoid metabolism and consequently anthocyanin accumulation and P-starvation were proven to be linked at a protein level. He et al. (2021) demonstrated that an inhibitor of the phosphate starvation response (SPX4) interacted with PAP1 (production of anthocyanin pigments) under P-sufficient conditions, while loss of this protein interaction under P-starvation resulted in induction of anthocyanin biosynthesis genes which proves the link between anthocyanin accumulation and P-starvation. This anthocyanin production is linked to the light energy captured during photosynthesis.

Under P stress, the light energy captured in the chloroplasts is higher than the capacity to process it, resulting in the inhibition of photosynthesis by light. In response to this photo-oxidative stress, the accumulation of anthocyanins in the vacuoles of epidermal cells can act as a photoprotectants (Gould *et al.*, 2008; Hernández and Munné-Bosch, 2015). Anthocyanins are synthesized through the phenylpropanoid pathway via an extension of the flavonoid pathway (Emiliani *et al.*, 2009; Zhang *et al.*, 2014). Here, we linked P deficiency in maize to the accumulation of anthocyanins and concomitant purple discoloration in leaves quantified through the mARI. The link between anthocyanins and mARI was previously shown by Gitelson *et al.* (2009). We confirmed the exponential relationship between plant P content and anthocyanin content as earlier described in tobacco (Li *et al.*, 2014; Fig. 1B), indicating anthocyanin accumulation is regulated through an on/off mechanism, which suggests that mARI can be used as a qualitative measure of P deficiency. Additionally, Fv/Fm values were negatively correlated with mARI, corroborating the photoprotective role of anthocyanin in maize leaves.

Despite the highly representative, exponential correlation between anthocyanin accumulation and P concentration established in maize plants and the recently proven molecular link between anthocyanin accumulation and P deficiency, the use of mARI as a proxy for P deficiency should be handled with care. For example, studies indicate that the addition of microbial products to *Arabidopsis* plants had an impact on gene regulation in the phenylpropanoid pathway and subsequent secondary metabolite production (Ali and McNear, 2014). Additionally, phytohormones such as auxins and gibberellins also play a role in the regulation of anthocyanin accumulation (Liu *et al.*, 2014; Hernández and Munné-Bosch, 2015). A specific case study is the non-pathogenic fungus *Cochliobolus heterostrophus*, which can reduce the expression of flavonoid-3-hydroxylase (F3H), dihydroflavanone 4-reductase (DFR) and anthocyanidin synthase (ANS), thereby decreasing anthocyanin accumulation (Lo and Nicholson, 1998). In this research, the addition of the fourth (enriched) consortium, V-B4, lead to a decoupling of anthocyanin accumulation and plant P content in maize, resulting in plants with a low mARI and low P contents. Therefore, the usefulness of the parameter mARI as a proxy for P deficiency can be compromised when treating plants with bacterial consortia, since certain specific bacteria and bacterial metabolites are able to interfere with the phenylpropanoid pathway and concomitant plant anthocyanin accumulation.

In vitro *parameters do not reflect a consortium's P-solubilizing effect on the plant*

When evaluating our *in planta* enriched bacterial suspensions *in vitro*, platings on LB and MPVK agar displayed a significantly lower amount of colony forming units in the RSS compared to the enrichments (V-B1-4). However, metagenomics analysis showed that species richness was significantly higher in the RSS compared to V-B1-4 which seems to be contradictory to the *in vitro* plating results. This observation can be explained by either the inability of certain bacterial species to grow on culturing media such as LB and MPVK, the slower growth rate of certain bacterial species, or the fact that the RSS' richness results from low count ASVs which might be easily outcompeted on culturing media by other species that exhibit rapid growth on these specific media (Tanaka *et al.*, 2014).

Since the most adopted strategy for screening potential PSB is the *in vitro* evaluation of bacterial isolates on selective growth media (Nautiyal, 1999; Rodrígez and Frage, 1999; Mehta and Nautiyal, 2001), we also evaluated the obtained bacterial consortia through this type of tests. *In vitro* screening of the mixed consortia gave no indications that a selection for bacterial suspensions with improved P-solubilizing traits was established. However, this approach neglects the paramount plant-bacteria interactions, as the ecological niche of the rhizosphere

environment is absent. Additionally, the bacterial consortium will consist of specific strains enriched for the P-solubilizing trait (*in planta*) on the one hand, but also of other non-P-solubilizing strains which might have thrived under the selective conditions by scavenging the released P. It is therefore possible that strains not capable of solubilizing P get the upper hand once introduced in bacterial growth medium. Finally, as we work with mixed bacterial suspensions instead of single isolates, we take bacteria–bacteria interactions into account (Pandey & Maheshwari, 2007; Venturi and Keel, 2016). The presence of some PSB can also cause a (partial) solubilization of insoluble phosphates, resulting in increased bio-available P for both themselves and other microorganisms present (Deubel and Merbach, 2005; Dai *et al.*, 2020). In the presence of a plant, the increased bio-available P can be used by both surrounding microorganisms and the host plant (Deubel and Merbach, 2005). In a plate assay, the effect of these bacterial interactions may increase the ability of different microorganisms to grow on the selective media resulting in a bacterial count equal to that on a rich (LB) medium.

Although we did not observe significant differences *in vitro*, we must note that the *in vitro* experiment was only performed in one specific environment (T, pH, growth medium). In future research, adaptations to these parameters could be included. For example, the addition of well-known root exudates to mimic the presence of a plant might influence a consortium's P-solubilizing capacity (Wang e*t al.*, 2021). Taking abovementioned observations into account, the *in vitro* evaluation of P-solubilization by the bacterial consortia obtained via the consecutive enrichments in our platform confirmed the shortcomings encountered in other *in vitro* studies aiming at selecting biostimulatory bacterial strains (Chauhan *et al.*, 2015; Souza *et al.*, 2015).

In planta *enrichment for P-solubilizing bacteria is coincided by a shift in bacterial populations in the Rhizosphere*

The microbial composition in the rhizosphere of maize is well documented. Previously performed metagenome studies indicate that Proteobacteria, Bacteroidetes, Actinobacteria and Firmicutes are amongst the most dominant phyla in the maize rhizosphere (Philippot *et al.*, 2013; Yang *et al.*, 2017). However, the composition of the rhizosphere microbiome alters according to plant age and developmental stage (Cavaglieri *et al.*, 2009; Chaparro *et al.*, 2014; Li *et al.*, 2019) and under abiotic stress (Beirinckx *et al.*, 2020). Furthermore, Chen et al. (2021) have described that PGPR inoculation may regulate the relative abundance of predominant bacteria in the rhizosphere and therefore readjusts the composition

and structure of the rhizosphere microbiome. In this research, we used maize grown till V5 stage to actively enrich microbes with the P-solubilization trait. The bacterial composition of the enriched suspensions was compared to that of the rhizosphere start suspension and existing literature. In general, the same bacterial phyla were found in the enriched suspensions as described in abovementioned literature, which indicates that, in the artificial sand:polymer system, plant–bacteria interactions comparable to interactions in a natural soil environment can be established. The most dominant phyla were those of the Proteobacteria and Bacteroidetes, presumably because of their fast growth rates and their ability to exploit transient niches for nutrition (Yang *et al.*, 2017). After *in planta* selection, already low abundant phyla such as Armatimonadetes and Gemmatimonadetes significantly decreased even more compared to the rhizosphere start suspension. In contrast, Cyanobacteria were significantly enriched from the start suspension, indicating that the *in planta* platform can be a leverage to enrich for low abundant phyla. Additionally, at each taxonomic level, we saw an increase of certain phyla (resp. classes, orders, families and genera), especially Proteobacteria, Bacteroidetes and Cyanobacteria, towards the third enrichment (V-B3), in which plants displayed the highest P contents. The V-B3 consortium therefore provides a valuable source of PSB, and possibly PGPR in general, from which single strains should be isolated and verified for their effectiveness in laboratory, pot and field trials.

In this study, a combination of iron and aluminium phosphate was used as sole P source. Amongst the few studies available describing successful iron and aluminium P-solubilizing microorganisms, the majority describes P-solubilizing fungi such as *Aspergillus* and *Penicillium* (Gadagi and Sa, 2002; Barroso and Nahas, 2007). Bacterial genera known to solubilize iron phosphate include *Azospirillum*, *Burkholderia* and *Pseudomonas* (Rosas *et al.*, 2006; Prijambada *et al.*, 2009; Reis *et al.*, 2011; Ghosh *et al.*, 2016). These genera belong to the orders of (resp.) the Azospirillales, Betaproteobacteriales and Pseudomonales, of which two out of three significantly increased in relative abundance after *in planta* enrichment.

A second shift in the microbial community co-occurs with a relapse in maize P status and an altered mARI response

The cyclic *in planta* enrichment for P-solubilizing bacteria was successful after three enrichments, resulting in healthier plants with P contents around 5000 mg P per kg dried material, which is the expected P content of young, healthy maize plants (Plank, 1989). This shift in

plant P content coincided with a shift in the bacterial rhizosphere composition. However, after a fourth enrichment, plants again displayed lower P contents and a second shift in bacterial composition was observed, ascribed to a recovery of Flavobacteriales (increased by 1.6-fold) and the Alphaproteobacteria Azospirillales and Rhizobiales (resp. increased by 2.8 and 1.7-fold). This reciprocal shift in bacterial community might suggest that, parallel to the enrichment for PSB, we also selected for other PGPR of which some possess N-fixing capacities.

Wright *et al.* (2019) described that, when artificially selecting microbial communities, the desired trait may be lost due to community succession. Optimal communities might rapidly decay due to their replacement by so-called cheaters and cross-feeders. One possibility is that, in this research, the increase in Azospirillales, Rhizobiales and Flavobacteriales disrupted the optimal P-solubilizing community by acting as cross-feeders.

Additionally, after passing a fourth enrichment, a decoupling of the mARI-phenotype and plant P status was observed. In this research, the second shift in bacterial community might result in the release of microbial metabolites able to interfere with the phenylpropanoid pathway as stated above. For example, one of the main modes of action of PGPR belonging to the genus *Azospirillum* is the production of the phytohormone indole-3-acetic acid and 1-aminocyclopropane-1-carboxylate deaminase (Walker *et al.*, 2011). Therefore, high abundances of *Azospirillum* might lead to a reduction of anthocyanin accumulation, even under low P levels in the plant, by interfering with the ternary complex of MYB-bHLH-WD40 transcription factors (MBW complex) (Petroni and Tonelli, 2011; Wang *et al.*, 2018a). However, this is one of multiple hypotheses and further research is necessary to fully understand the plant–bacterial interactions leading to the delayed or repressed accumulation of anthocyanins due to P stress.

Elaborating on this matter, a functional metagenomics and metatranscriptomics study may be interesting for studying gene functions in the consortia. However, P-solubilization can be mediated through a number of genes, amongst which the genes involved in inorganic P-solubilization and organic P mineralization (*gcd*, *phoD*, *phoA*, *appA*, *phn*); non-specific acid phosphatases (NSAPs; class A, B and C NSAP genes); P uptake and transport genes (*pst*, *pit*); P-starvation response (*phoU*, *phoR*, *phoB*) (Neal *et al.*, 2018; Dai *et al.*, 2020; Udaondo *et al.*, 2020); PQQ biosynthetic genes (Ludueña *et al.*, 2017); but also (amongst others) genes involved in siderophore production, for example enterobactin (*EntD, EntF, EntC, EntE, EntB* and *EntA*) (Shariati *et al.*, 2017).

Concluding remarks

Through the *in planta* enrichment platform, in which maize was consecutively exposed to insoluble phosphorus, we succeeded to enrich the rhizosphere for a rhizosphere competent, P-solubilizing consortium. Inoculated maize grown under P limitation showed an improved P status by the third consecutive enrichment over non-inoculated plants, which coincided with a shift in the rhizosphere community. This third bacterial suspension comprises bacterial groups that are typically associated with plant growth promotion (specifically P-solubilization) and can be used as a valuable source for the *in vitro* isolation of single strains, to be subsequently evaluated *in planta*. Although metabarcoding could not ascribe specific taxa to the trait of interest, a functional metagenomics analysis may assign specific gene expression to the enriched consortia.

In this research, it became apparent that the conventional *in vitro* screening methods for PSB did not produce an adequate representation of their *in planta* performance. Additionally, when using the *in planta* enrichment platform, the number of enrichments is an important factor to take into account as, in this research, prolonged enrichment led to a second shift in rhizosphere community which differentially affected the P status in maize.

Experimental procedures

Microbial substrates

Lysogeny broth (LB) agar was used as a rich solid medium (Table S2) (Bertani, 1951). Modified Pikovskaya agar (MPVK) was used as a selective solid medium for the assessment of P-solubilization and organic acid production (Table S2) (Gupta *et al.*, 1994; Chatli *et al.*, 2008; Soni *et al.*, 2013). In the MPVK agar, a 1:1 mole-mixture of iron(III)phosphate ($FePO_4.2H_2O$) and aluminium phosphate ($AlPO_4$) was used as an insoluble P source. National Botanical Research Institute's Phosphate (NBRIP) growth medium with $FePO_4.2H_2O$ and $AlPO_4$ in a 1:1 mole ratio as insoluble P source (further referred at as NBRIP-*FeP:AlP*) was used as a selective medium to grow microorganisms (Table S2) (Nautiyal, 1999).

Bacterial isolation and growth conditions

Rhizosphere samples from maize plants were obtained from five different locations in Flanders (Table S3). Each site was sampled at three different locations within the field by removing the entire plant root system with a shovel, followed by gently removing the bulk soil. The root tips (1-2 cm) with adhering rhizosphere soil were

collected, pooled and shaken in sterile saline solution (0.85% NaCl (w:v)) in a 1:10 (w:v) ratio at 140 rpm for 1 h. Aliquots of this rhizosphere start suspension (RSS) were archived in vials containing 23% glycerol at −80°C (Fig. 6: RSS). Subsequently, the bacterial suspension was inoculated in liquid NBRIP-*FeP:AlP* medium (Nautiyal, 1999) and incubated at room temperature (21°C) in the dark for 5 days. After incubation, bacterial suspensions were washed in saline solution by centrifuging the suspension at 1500 rpm for 90 s after which the cell containing supernatant was transferred to a second sterile recipient and was washed three times by centrifuging 10 min at 4000 rpm, gently removing the supernatant and re-suspending the bacterial pellet in saline solution. The entire process of rhizosphere sampling, bacterial isolation, storage and growth was performed analogously in the enrichment experiments (see below).

DNA extraction and 16S metabarcoding

Rhizosphere bacteria were collected from the roots in saline solution as mentioned above. DNA was extracted from 250 μl of the bacterial suspensions using the DNeasy® PowerSoil® Kit (Qiagen, Hilden, Germany). The bacterial V3 and V4 regions of the 16S rRNA gene were amplified by using the primer pair S-D-Bact-0341-b-S-17/S-D-Bact-0785-a-A-21 (Klindworth *et al.*, 2013), extended with Illumina specific adaptors. A second PCR (index PCR) was performed to attach dual indices and Illumina sequencing adaptors using the Nextera XT Index Kit (Illumina, San Diego, CA, USA). PCR conditions were used as described by Debode *et al.* (2016). PCR mastermixes were prepared using KAPA HiFi HotStart ReadyMix (Kapa Biosystems, Wilmington, MA, USA) according to the manufacturer's instructions. Each PCR was followed by a PCR clean-up using HighPrep PCR beads (MAGBIO, Gaithersburg, MA, USA). The final PCR products were controlled for their quality via the QIAxcel Advanced system with the QIAxcel DNA High Resolution kit (QIAGEN, Germantown, MD, USA), and concentrations were measured using the Quantus double-stranded DNA assay (Promega, Madison, WI, USA). The final barcoded libraries were diluted to 10 nM, equally pooled and sequenced on an Illumina MiSeq system (2 × 300bp) by Admera (South Plainfield, NJ, USA).

Sequence processing and downstream analysis of the ASV table

Demultiplexing of the amplicon data set and barcode removal was done by the sequencing provider. Primers were removed using Trimmomatic v0.32 (Bolger *et al.*, 2014). Trimming, filtering, merging of the reads, dereplication, sorting, amplicon sequence variant (ASV) calling and chimera removal was done making use of the DADA2 algorithm v1.12 (Callahan *et al.*, 2016). Briefly, all ambiguous bases were removed and the number of maximum expected errors for forward and reverse reads should not exceed three or five respectively. A
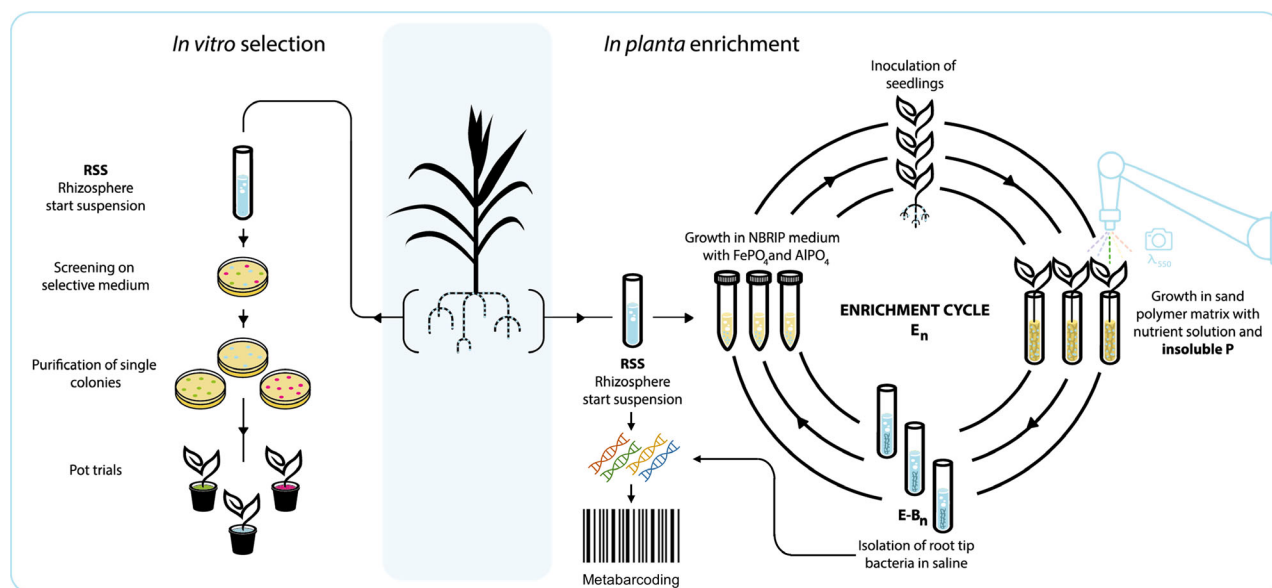

Fig. 6. Overview of the current screening and selection technique for plant growth-promoting rhizobacteria (PGPR) (left panel) versus our newly presented *in planta* enrichment platform for the selection of PGPR (right panel). RSS: Rhizosphere start suspension; E-Bn: bacterial suspension isolated from enrichment *n*.

parametric error model was built for the forward and reverse read separately, for which convergence was reached after eight and six rounds. After dereplication, reads were merged and an ASV table was built. To assign taxonomy through the decipher library (v2.12.0) to the resulting ASVs, the SILVA database v132 (Quast *et al.*, 2012) for the V3-V4 16S rRNA gene sequences was used as a reference. The resulting count table was used for statistical analysis.

Bacterial P-solubilizing assay

Bacterial suspensions were tested for their P-solubilizing capacity in NBRIP-*FeP:AlP* medium. After 5 days of growth, samples were collected and centrifuged at 5000 rpm for 10 min to separate bacteria and insoluble phosphates from soluble phosphates. Soluble phosphates were determined by an adaptation of the colorimetric method of Fiske and Subbarow (1925) by adding 15% (w:v) ammonium molybdate (in a 5.5% (v:v) H_2SO_4 solution) to the samples in a 1 : 1 (v:v) ratio (Magallón-Servin, 2014). The phosphomolybdate produced was measured spectrophotometrically at 405 nm against a standard curve prepared with KH_2PO_4 ranging from 0 to 40 mg P l^{-1}.

Quantification of organic acid production

Organic acid production was evaluated on MPVK agar with a pH indicator (bromophenol blue). Pictures of the MPVK plates were captured, and the RGB images were evaluated with Phenovation Data Analysis V5.5.1. Per image, individual pixels were evaluated for their RGB values and divided into two classes: class I containing all pixels in the yellow spectrum and class II containing all other pixels.

Plant material and growth substrate

Untreated maize (*Zea mays* L.) seeds (hybrid var. LG 30.217; Limagrain, Kerkhove, Belgium) were surface sterilized for 3 min in a 5% sodium hypochlorite solution (Simons *et al.*, 1996). Seeds were rinsed five times by soaking them in sterile distilled water and subsequently germinated in sterile vermiculite for 7 days at 21°C under sun LED modules (SLMs) (Phenovation, Wageningen, The Netherlands) with a light : dark cycle of 15 h : 9 h.

A mixture of washed, non-sterile fine quartz sand (Vosschemie Benelux, Lier, Belgium) and a water-absorbent synthetic polymer (DCM Aquaperla®, Grobbendonk, Belgium) was used as growth substrate. The polymer was added to distilled water in a 1 : 100 (w:v) ratio, set to form a gel for 2 h and was subsequently mixed with fine sand in a 1.5 : 10 (v:w) ratio and air-dried for 7 days (Kyndt *et al.*, 2017). The pH of this growth substrate is 7.2.

In planta *enrichment procedure for PSB*

Compared to the commonly used *in vitro* platform (Fig. 6, left), the cyclic *in planta* enrichment platform encompasses plant–bacteria interactions already from the first stage of PSB selection (Fig. 6, right). A rhizosphere start suspension was used to inoculate untreated maize seedlings with the aim to selectively enrich for highly effective root colonizing and P-solubilizing microorganisms (Fig. 2A). Six independent replicate lines were set up, which were enriched through three enrichments, and each enriched bacterial suspension was stored at −80°C (Fig. 2A, E-B1-3). The stored bacterial suspensions were evaluated in an overall validation experiment.

Plants were grown in glass test tubes (diameter 38 mm, height 200 mm) with 240 g of growth substrate and roots were protected from light. The P dose applied to the growth substrate was determined based on the minimal P concentration for maize growth (10 mg kg^{-1}) as described in Deng *et al.* (2014) and Redi *et al.* (2016). A mixture of $FePO_4.2H_2O$ and $AlPO_4$ (1:1 mole ratio) was used as an insoluble P source and was mixed as a powder (per recipient: $FePO_4.2H_2O$, 0.121 g; $AlPO_4$, 0.079 g) with the growth substrate. Within 1 cm of the seedlings' roots, the bacterial suspensions were inoculated by adding 1 ml of liquid inoculum at OD_{600} 0.6. Tubes were incubated in a controlled environment (T 21°C; RH 40%; 255.5 µmol (m^2 s)$^{-1}$ photosynthetically active radiation (PAR); light : dark, 15 h : 9 h) and were irrigated with a modified Hoagland solution (Table S4) (Hoagland and Arnon, 1950; Cooper and Burton, 2004). Plants were grown over a time period of 21 days followed by rhizosphere sampling and bacterial isolation from the rhizosphere as described above. The experiments comprised a positive and a negative control (plants supplied with KH_2PO_4; resp. plants supplied with insoluble FeP:AlP; Table S4) to evaluate the plant P status parameters (mARI and P content) against.

Plant growth was monitored every 3 days. At the end of the experiment, roots were sampled and bacteria were isolated from the rhizosphere; shoot fresh and dry weights were determined. Drying occurred at 60°C for 48 h. In addition, rhizosphere colonization was determined by plating rhizosphere samples on both rich (LB) and selective (MPVK) agar through the method of Miles et al. (1938).

Visualization of P deficiency using multispectral imaging

To automatically measure the phosphorus and health status of the maize plants, we used a multispectral

imaging platform. The platform allows to visualize diverse physiological traits in real time, based on specific absorption, reflection and emission patterns. The central part of the platform comprises a 3CCD 6Mp-16 bit camera mounted on a Cartesian coordinate robot, equipped with 12 optical interference filters (CropReporter, Phenovation, Wageningen, The Netherlands).

The efficiency of photosystem II in a dark adapted state (PSII; Fv/Fm) (Baker, 2008) was measured according to the manufacturer's specifications and the modified anthocyanin reflectance index (mARI) was determined using following formula (Gitelson *et al.*, 2009):

$$mARI = \left(\frac{1}{\rho_{550nm}} - \frac{1}{\rho_{710nm}}\right)\rho_{770nm}, \qquad (2)$$

where ρ_{550} is the reflectance in the first spectral band, which is maximally sensitive to anthocyanin content; ρ_{710} the reflectance in the second spectral band, which is maximally sensitive to chlorophyll content but not sensitive to anthocyanin content; and ρ_{770} the reflectance of the third spectral band, which compensates for leaf thickness and density.

To validate mARI as a proxy for P deficiency, the correlation between mARI and anthocyanin was established in maize. In a separate experiment, maize plants were grown in a controlled environment (T 21°C, 255.5 μmol $(m^2 \ s)^{-1}$ PAR, light : dark 15 h : 9 h) under five different P concentrations (0.0, 0.7, 1.4, 3.5, 7.0 mg P per plant) over a time period of 21 days. The mARI of an 8 cm long piece from the centre of the 2nd and 3rd youngest leaf was measured, and anthocyanins were extracted as described by Pietrini *et al.* (2002) and measured spectrophotometrically as described by Mancinelli *et al.* (1975).

In the *in planta* enrichment experiment, mARI was measured both using a longitudinal approach on intact plants (from day 10 after inoculation onwards) and on detached leaf pieces at the end of the experiment. In the longitudinal images, the mARI was computed based on a region of interest (ROI) of 200×200 pixels on a non-overlapping leaf. End-point measurements were performed on an 8 cm long piece from the centre of the 3rd youngest leaf, for which mARI values obtained for each pixel were averaged.

Plant nutrient content

The phosphorus and potassium contents of the plant material were determined through inductively coupled plasma optical emission spectrometry (ICP-OES). Dried shoot material was fractionated and incinerated in a muffle furnace at 500°C for 4 h, followed by two digestion steps in 6 M and 3 M HCl respectively. Digested

samples were diluted with ultrapure water and filtered through a Whatman® n°5 filter to remove carbon remnants. Additionally, the plant nitrogen content was determined via the Dumas method (Dumas, 1831).

Statistics

Statistical analysis on the ASV table was done in RStudio version 3.5.1 (R Core Team, 2018). For each sample, species richness (Chao1; package *'OTUtable'*; Linz, 2018), diversity (H, Shannon index; package *'vegan'*; Oksanen et al., 2019) and evenness (J, Pielou's evenness; *H/log(S), where S = n° of species*) were determined, grouped per treatment and differences were statistically evaluated with ANOVA and *post hoc* tests after verifying data normality and homoscedasticity (Tukey or Dunnett T3). Taxa were analysed using the *'phyloseq'* package (McMurdie and Holmes, 2013). Bacterial abundances of the rhizosphere start suspension were compared to the enriched suspensions by clustering the ASV table (merge phyla, resp. class, order and family). Differential abundances were assessed using likelihood-ratio tests as described in detail in De Tender *et al.* (2016) by using the *edgeR* package version 3.12.0 (Robinson *et al.*, 2010). Bacterial abundances were normalized by only keeping those phyla (resp. classes, orders, family) which were present with a minimal abundance of 0.05% in at least six samples. Plant parameters were correlated to bacterial abundances by means of Spearman correlations (packages *'Hmisc'* and *'corrplot'*; Harrell, 2020; Wei *et al.*, 2017). Finally, the metagenomics data were coupled to the plant parameters and the combined (Hellinger transformed) ASV table was used to conduct PERMANOVA statistics on the Bray–Curtis distances to test biological differences due to grouping variables (functions *'adonis'*, *'decostand'* and *'vegdist'*, package *'vegan'*; Oksanen *et al.*, 2019). PERMANOVA was executed after checking homogeneity of variances with the betadisper function. To illustrate these biological differences, principal component analysis (PCA) using the *'factoextra'* package (Kassambara and Mundt, 2020) was performed.

The *in planta* data and image data were statistically analysed using IBM SPSS statistics, version 25.0 (Armonk, NY, USA). Treatments and controls were statistically compared through one-way ANOVA followed by a *post hoc* Tukey test. Normality and homoscedasticity assumptions were verified using diagnostic plots. In the rare case of strong violation of the homoscedasticity assumption, a Welch correction was applied and the Dunnet's T3 test was used as *post hoc* test. All hypotheses were tested at a 5% significance level.

Acknowledgements

Funding Information

Conflict of interest

None declared.

Authors' contributions

KA, LDG, MA and NDZ provided the concept and experimental design of the research; NDZ performed the experiments; PV performed the chemical nutrient analysis; SO and NDZ conducted the amplicon sequencing, bio-informatics and statistical analysis of the NGS data in cooperation with JD and CDT; other data were processed and analysed by JV, MA, KA and NDZ; NDZ prepared the manuscript; KA, MA and LDG supervised the manuscript; all authors revised the manuscript.

References

Ali, M.B., and **McNear**, D.H. (2014) Induced transcriptional profiling of phenylpropanoid pathway genes increased flavonoid and lignin content in Arabidopsis leaves in response to microbial products. *BMC Plant Biol* **14:** 84.

Amaya-Gómez, C.V., Porcel, M., Mesa-Garriga, L., and Gómez-Álvarez, M.I. (2020) A framework for the selection of plant growth-promoting rhizobacteria based on bacterial competence mechanisms. *Appl Environ Microbiol* **86:** e00760–e00820.

Amery, F., and Vandecasteele, B. (2015) *Wat weten we over fosfor en landbouw? Deel 1 Beschikbaarheid van fosfor in bodem en bemesting*. Flanders Institute for Agriculture, Fisheries and Food. ILVO Mededeling 195.

Armanhi, J.S.L., de Souza, R.S.C., Damasceno, N.D.B., de Araújo, L.M., Imperial, J., and Arruda, P. (2018) A Community-based culture collection for targeting novel plant growth-promoting bacteria from the sugarcane microbiome. *Front Plant Sci* **8:** 2191.

Babalola, O.O. (2010) Beneficial bacteria of agricultural importance. *Biotech Lett* **32:** 1559–1570.

Bach, E., dos Santos Seger, G.D., de Carvalho Fernandes, G., Lisboa, B., and Passaglia, L.M.P. (2016) Evaluation of biological control and rhizosphere competence of plant growth promoting bacteria. *Appl Soil Ecol* **99:** 141–149.

Backer, R., Rokem, J.S., Ilangumaran, G., Lamont, J., Praslickova, D., Ricci, E., *et al.* (2018) Plant growth-promoting rhizobacteria: context, mechanisms of action, and roadmap to commercialization of biostimulants for sustainable agriculture. *Front Plant Sci* **9:** 1473.

Bais, H.P., Weir, T.L., Perry, L.G., Gilroy, S., and Vivanco, J.M. (2006) The role of root exudates in rhizosphere interactions with plants and other organisms. *Annu Rev Plant Biol* **57:** 233–266.

Baker, N.R. (2008) Chlorophyll fluorescence: a probe of photosynthesis in vivo. *Ann Rev Plant Biol* **59:** 89–113.

Barea, J.M., Pozo, M.J., Azcon, R., and Azcon-Aguilar, C. (2005) Microbial co-operation in the rhizosphere. *J Exp Bot* **56:** 1761–1778.

Barroso, C.B., and Nahas, E. (2007) Solubilization of hardly soluble iron and aluminum phosphates by the fungus Aspergillus niger in the soil. In: *First International Meeting on Microbial Phosphate Solubilization*. Dordrecht: Springer, pp. 193–198.

Bashan, Y., Kamnev, A.A., and de-Bashan, L.E. (2013) Tricalcium phosphate is inappropriate as a universal selection factor for isolating and testing phosphate-solubilizing bacteria that enhance plant growth: a proposal for an alternative procedure. *Biol Fertil Soils* **49:** 465–479.

Beirinckx, S., Viaene, T., Haegeman, A., Debode, J., Amery, F., Vandenabeele, S., *et al.* (2020) Tapping into the maize root microbiome to identify bacteria that promote growth under chilling conditions. *Microbiome* **8:** 1–13.

Benizri, E., Baudoin, E., and Guckert, A. (2001) Root colonization by inoculated plant growth-promoting rhizobacteria. *Biocontrol Sci Tech* **11:** 557–574.

Bertani, G. (1951) Studies on lysogenesis I.: the mode of phage liberation by lysogenic *Escherichia coli*. *J Bacteriol* **62:** 293.

Bhattacharyya, P.N., and Jha, D.K. (2012) Plant growth-promoting rhizobacteria (PGPR): emergence in agriculture. *World J Microbiol Biotechnol* **28:** 1327–1350.

Bolger, A.M., Lohse, M., and Usadel, B. (2014) Trimmomatic: a flexible trimmer for Illumina sequence data. *Bioinformatics* **30:** 2114–2120.

Callahan, B.J., McMurdie, P.J., Rosen, M.J., Han, A.W., Johnson, A.J.A., and Holmes, S.P. (2016) DADA2: high-resolution sample inference from Illumina amplicon data. *Nat Methods* **13:** 581.

Castrillo, G., Teixeira, P.J.P.L., Paredes, S.H., Law, T.F., de Lorenzo, L., Feltcher, M.E., *et al.* (2017) Root microbiota drive direct integration of phosphate stress and immunity. *Nature* **543:** 513.

Cavaglieri, L., Orlando, J., and Etcheverry, M. (2009) Rhizosphere microbial community structure at different maize plant growth stages and root locations. *Microbiol Res* **164:** 391–399.

Chaparro, J.M., Badri, D.V., and Vivanco, J.M. (2014) Rhizosphere microbiome assemblage is affected by plant development. *ISME J* 8: 790–803.

Chatli, A.S., Beri, V., and Sidhu, B.S. (2008) Isolation and characterisation of phosphate solubilising microorganisms from the cold desert habitat of Salix alba Linn. in trans Himalayan region of Himachal Pradesh. *Ind J Microbiol* 48: 267–273.

Chauhan, H., Bagyaraj, D.J., Selvakumar, G., and Sundaram, S.P. (2015) Novel plant growth promoting rhizobacteria—Prospects and potential. *Appl Soil Ecol* 95: 38–53.

Chen, L., Hao, Z., Li, K., Sha, Y., Wang, E., Sui, X., *et al.* (2021) Effects of growth-promoting rhizobacteria on maize growth and rhizosphere microbial community under conservation tillage in Northeast China. *Microb Biotechnol* 14: 535–550.

Compant, S., Clément, C., and Sessitsch, A. (2010) Plant growth-promoting bacteria in the rhizo-and endosphere of plants: their role, colonization, mechanisms involved and prospects for utilization. *Soil Biol Biochem* 42: 669–678.

Cooper, E.L., and Burton, L.D. (2004) *Agriscience: Fundamentals & Applications*, 3rd edn. Boston, MA: Thomson Learning.

Cordell, D., Drangert, J.O., and White, S. (2009) The story of phosphorus: global food security and food for thought. *Glob Environ Change* 19: 292–305.

Dai, Z., Liu, G., Chen, H., Chen, C., Wang, J., Ai, S., *et al.* (2020) Long-term nutrient inputs shift soil microbial functional profiles of phosphorus cycling in diverse agroecosystems. *ISME J* 14: 757–770.

Dakora, F.D., and Phillips, D.A. (2002) Root exudates as mediators of mineral acquisition in low-nutrient environments. In: *Food Security in Nutrient-Stressed Environments: Exploiting Plants' Genetic Capabilities*. Dordrecht: Springer, pp. 201–213.

De Tender, C., Haegeman, A., Vandecasteele, B., Clement, L., Cremelie, P., Dawyndt, P., *et al.* (2016) Dynamics in the strawberry rhizosphere microbiome in response to biochar and Botrytis cinerea leaf infection. *Front Microbiol* 7: 2062.

Debode, J., De Tender, C., Soltaninejad, S., Van Malderghem, C., Haegeman, A., Van der Linden, I., *et al.* (2016) Chitin mixed in potting soil alters lettuce growth, the survival of zoonotic bacteria on the leaves and associated rhizosphere microbiology. *Front Microbiol* 7: 565.

Deng, Y., Chen, K., Teng, W., Zhan, A.i., Tong, Y., Feng, G.u., *et al.* (2014) Is the inherent potential of maize roots efficient for soil phosphorus acquisition? *PLoS One* 9: e90287.

Deubel, A., and Merbach, W. (2005) Influence of microorganisms on phosphorus bioavailability in soils. *Microorganisms in Soils: Roles in Genesis and Functions*. Berlin, Heidelberg: Springer, pp. 177–191.

Dumas, J.B.A. (1831) Procedes de l'analyse organique. *Annales de Chimie et de Physique* 47: 198–205.

Emiliani, G., Fondi, M., Fani, R., and Gribaldo, S. (2009) A horizontal gene transfer at the origin of phenylpropanoid metabolism: a key adaptation of plants to land. *Biology Direct* 4: 7.

Etesami, H., Mirsyed Hosseini, H., and Alikhani, H.A. (2014) *In planta* selection of plant growth promoting endophytic bacteria for rice (*Oryza sativa* L.). *J Soil Sci Plant Nutri* 14: 491–503.

Fiske, C.H., and Subbarow, Y. (1925) The colorimetric determination of phosphorus. *J Biol Chem* 66: 375–400.

Gadagi, R.S., and Sa, T. (2002) New isolation method for microorganisms solulbilizing iron and aluminum phosphates using dyes. *Soil Sci Plant Nutri* 48: 615–618.

Ghosh, R., Barman, S., Mukherjee, R., and Mandal, N.C. (2016) Role of phosphate solubilizing Burkholderia spp. for successful colonization and growth promotion of *Lycopodium cernuum* L. (Lycopodiaceae) in lateritic belt of Birbhum district of West Bengal, India. *Microbiol Res* 183: 80–91.

Gitelson, A.A., Chivkunova, O.B., and Merzlyak, M.N. (2009) Nondestructive estimation of anthocyanins and chlorophylls in anthocyanic leaves. *Am J Bot* 96: 1861–1868.

Gould, K., Davies, K.M., and Winefield, C. (Eds.), (2008) *Anthocyanins: Biosynthesis, Functions, and Applications*. Berlin, Germany: Springer Science & Business Media.

Guo, X., Duan, X., Wu, Y., Cheng, J., Zhang, J., Zhang, H., and Li, B. (2018) Genetic engineering of maize (*Zea mays* L.) with improved grain nutrients. *J Agricult Food Chem* 66: 1670–1677.

Gupta, R., Singal, R., Shankar, A., Kuhad, R.C., and Saxena, R.K. (1994) A modified plate assay for screening phosphate solubilizing microorganisms. *J Gen Appl Microbiol* 40: 255–260.

Gwirtz, J.A., and Garcia-Casal, M.N. (2014) Processing maize flour and corn meal food products. *Ann N Y Acad Sci* 1312: 66–75.

Harrell, F. E. (2020) *Hmisc: Harrell Miscellaneous. R package Version 4.4-0*. URL https://cran.r-project.org/web/packages/Hmisc/index.html.

He, Y., Zhang, X., Li, L., Sun, Z., Li, J., Chen, X., and Hong, G. (2021) SPX4 interacts with both PHR1 and PAP1 to regulate critical steps in phosphorus-status-dependent anthocyanin biosynthesis. *New Phytol* 230: 205–217.

Hernández, I., and Munné-Bosch, S. (2015) Linking phosphorus availability with photo-oxidative stress in plants. *J Exp Bot* 66: 2889–2900.

Hoagland, D.R., and Arnon, D.I. (1950) The water-culture method for growing plants without soil. In *Circular. California Agricultural Experiment Station 347*, 2nd edn. Berkeley, CA: College of Agriculture, University of California.

Jiang, C., Gao, X., Liao, L., Harberd, N.P., and Fu, X. (2007) Phosphate starvation root architecture and anthocyanin accumulation responses are modulated by the gibberellin-DELLA signaling pathway in Arabidopsis. *Plant Physiol* 145: 1460–1470.

Kai, M., Effmert, U., and Piechulla, B. (2016) Bacterial-plant-interactions: approaches to unravel the biological function of bacterial volatiles in the rhizosphere. *Front Microbiol* 7: 108.

Kamilova, F., Validov, S., Azarova, T., Mulders, I., and Lugtenberg, B. (2005) Enrichment for enhanced competitive plant root tip colonizers selects for a new class of biocontrol bacteria. *Environ Microbiol* 7: 1809–1817.

Kassambara, A., and Mundt, F. (2020) *factoextra: Extract and Visualize the Results of Multivariate Data Analysis*. R package Version 1.0.7. URL https://cran.r-project.org/web/packages/factoextra/index.html.

Khan, A.A., Jilani, G., Akhtar, M.S., Naqvi, S.M.S., and Rasheed, M. (2009) Phosphorus solubilizing bacteria: occurrence, mechanisms and their role in crop production. *J Agricult Biol Sci* **1:** 48–58.

Khan, M.S., Zaidi, A., and Wani, P.A. (2007) Role of phosphate solubilizing microorganisms in sustainable agriculture-a review. *Agron Sustain Dev* **27:** 29–43.

Klindworth, A., Pruesse, E., Schweer, T., Peplies, J., Quast, C., Horn, M., and Glöckner, F.O. (2013) Evaluation of general 16S ribosomal RNA gene PCR primers for classical and next-generation sequencing-based diversity studies. *Nucleic Acids Res* **41:** e1.

Kuiper, I., Bloemberg, G.V., and Lugtenberg, B.J. (2001) Selection of a plant-bacterium pair as a novel tool for rhizostimulation of polycyclic aromatic hydrocarbon-degrading bacteria. *Mol Plant Microbe Interact* **14:** 1197–1205.

Kyndt, T., Nahar, K., Haeck, A., Verbeek, R., Demeestere, K., and Gheysen, G. (2017) Interplay between carotenoids, abscisic acid and jasmonate guides the compatible rice-*Meloidogyne graminicola* interaction. *Front Plant Sci* **8:** 951.

Lebeis, S.L., Rott, M., Dangl, J.L., and Schulze-Lefert, P. (2012) Culturing a plant microbiome community at the cross-Rhodes. *New Phytol* **196:** 341–344.

Li, H., Ding, X., Chen, C., Zheng, X., Han, H., Li, C., *et al.* (2019) Enrichment of phosphate solubilizing bacteria during late developmental stages of eggplant (*Solanum melongena* L.). *FEMS Microbiol Ecol* **95:** fiz023.

Li, Y., Gu, M., Zhang, X., Zhang, J., Fan, H., Li, P., *et al.* (2014) Engineering a sensitive visual-tracking reporter system for real-time monitoring phosphorus deficiency in tobacco. *Plant Biotechnol J* **12:** 674–684.

Linz, A. (2018) *OTUtable: North Temperate Lakes - Microbial Observatory 16S Time Series Data and Functions*. R package Version 1.1.2. URL https://cran.r-project.org/web/packages/OTUtable/index.html.

Liu, M., Liu, X.u., Cheng, B.-S., Ma, X.-L., Lyu, X.-T., Zhao, X.-F., *et al.* (2016) Selection and evaluation of phosphate-solubilizing bacteria from grapevine rhizospheres for use as biofertilizers. *Span J Agricult Res* **14:** 26.

Liu, Z., Shi, M.Z., and Xie, D.Y. (2014) Regulation of anthocyanin biosynthesis in *Arabidopsis thaliana* red pap1-D cells metabolically programmed by auxins. *Planta* **239:** 765–781.

Lo, S.C.C., and Nicholson, R.L. (1998) Reduction of light-induced anthocyanin accumulation in inoculated sorghum mesocotyls: implications for a compensatory role in the defense response. *Plant Physiol* **116:** 979–989.

Ludueña, L.M., Anzuay, M.S., Angelini, J.G., Barros, G., Luna, M.F., Monge, M.D.P., *et al.* (2017) Role of bacterial pyrroloquinoline quinone in phosphate solubilizing ability and in plant growth promotion on strain *Serratia* sp. S119. *Symbiosis* **72:** 31–43.

Lynch, J. M., and de Leij, F. (2001) *Rhizosphere. e LS.*

Magallón-Servin, P. (2014) *Development of an inoculant of phosphate rock-solubilizing bacteria to improve maize growth and nutrition*. PhD thesis, Université Laval, Québec, Canada.

Mancinelli, A.L., Yang, C.P.H., Lindquist, P., Anderson, O.R., and Rabino, I. (1975) Photocontrol of anthocyanin synthesis: III. The action of streptomycin on the synthesis of chlorophyll and anthocyanin. *Plant Physiol* **55:** 251–257.

McMurdie, P.J., and Holmes, S. (2013) phyloseq: an R package for reproducible interactive analysis and graphics of microbiome census data. *PLoS One* **8:** e61217.

Mehta, S., and Nautiyal, C.S. (2001) An efficient method for qualitative screening of phosphate-solubilizing bacteria. *Curr Microbiol* **43:** 51–56.

Miles, A.A., Misra, S.S., and Irwin, J.O. (1938) The estimation of the bactericidal power of the blood. *Epidemiol Infect* **38:** 732–749.

Nautiyal, C.S. (1999) An efficient microbiological growth medium for screening phosphate solubilizing microorganisms. *FEMS Microbiol Lett* **170:** 265–270.

Neal, A.L., Blackwell, M., Akkari, E., Guyomar, C., Clark, I., and Hirsch, P.R. (2018) Phylogenetic distribution, biogeography and the effects of land management upon bacterial non-specific Acid phosphatase Gene diversity and abundance. *Plant Soil* **427:** 175–189.

Oksanen, J., Blanchet, F. G., Friendly, M., Kindt, R., Legendre, P., McGlinn, D., *et al.* (2019) *vegan: Community Ecology Package. R package Version 2.5-6*. URL https://cran.r-project.org/web/packages/vegan/index.html.

Oldroyd, G.E. (2013) Speak, friend, and enter: signalling systems that promote beneficial symbiotic associations in plants. *Nat Rev Microbiol* **11:** 252.

Osborne, S.L., Schepers, J.S., Francis, D.D., and Schlemmer, M.R. (2002) Detection of phosphorus and nitrogen deficiencies in corn using spectral radiance measurements. *Agron J* **94:** 1215–1221.

Pandey, P., and Maheshwari, D.K. (2007) Two-species microbial consortium for growth promotion of Cajanus cajan. *Curr Sci* **92:** 1137–1142.

Petroni, K., and Tonelli, C. (2011) Recent advances on the regulation of anthocyanin synthesis in reproductive organs. *Plant Sci* **181:** 219–229.

Philippot, L., Raaijmakers, J.M., Lemanceau, P., and Van Der Putten, W.H. (2013) Going back to the roots: the microbial ecology of the rhizosphere. *Nat Rev Microbiol* **11:** 789–799.

Pietrini, F., Iannelli, M.A., and Massacci, A. (2002) Anthocyanin accumulation in the illuminated surface of maize leaves enhances protection from photo-inhibitory risks at low temperature, without further limitation to photosynthesis. *Plant, Cell Environ* **25:** 1251–1259.

Pii, Y., Mimmo, T., Tomasi, N., Terzano, R., Cesco, S., and Crecchio, C. (2015) Microbial interactions in the rhizosphere: beneficial influences of plant growth-promoting rhizobacteria on nutrient acquisition process. A review. *Biol Fertil Soils* **51:** 403–415.

Plank, C.O. (1989) *Plant Analysis Handbook for Georgia*. Hall Athens, GA: Cooperative Extension Service, University of Georgia College of Agriculture.

Prijambada, I.D., Widada, J., Kabirun, S., and Widianto, D. (2009) Secretion of organic acids by phosphate solubilizing bacteria. *J Trop Soils* **14:** 245–251.

Quast, C., Pruesse, E., Yilmaz, P., Gerken, J., Schweer, T., Yarza, P., *et al.* (2012) The SILVA ribosomal RNA gene database project: improved data processing and web-based tools. *Nucleic Acids Res* **41:** D590–D596.

R Core Team (2018) *R: A Language and Enviroment for Statistical Computing*. Vienna, Austria: R Foundation for Statistical Computing. https://www.R-project.org

Raaijmakers, J.M., Paulitz, T.C., Steinberg, C., Alabouvette, C., and Moënne-Loccoz, Y. (2009) The rhizosphere: a playground and battlefield for soilborne pathogens and beneficial microorganisms. *Plant Soil* **321:** 341–361.

Raghothama, K.G. (2000) Phosphate transport and signaling. *Curr Opin Plant Biol* **3:** 182–187.

Redi, M., Gebremedhin, W., Merkeb, F., and Yimam, M. (2016) Critical level of extractable phosphorus for maize (*Zea mays* L.) at Metekel zone, Northwestern Ethiopia. *World Sci News* **54:** 14–26.

Reijnders, L. (2014) Phosphorus resources, their depletion and conservation, a review. *Resour Conserv Recycl* **93:** 32–49.

Reis, V.M., dos Santos Teixeira, K.R., and Pedraza, R.O. (2011) What is expected from the genus Azospirillum as a plant growth-promoting bacteria? In *Bacteria in Agrobiology: Plant Growth Responses*. Berlin, Heidelberg: Springer, pp. 123–138.

Reuter, H.I., Lado, L.R., Hengl, T., and Montanarella, L. (2008) Continental-scale digital soil mapping using European soil profile data: soil pH. *Hamburger Beiträge zur Physischen Geographie und Landschaftsökologie* **19:** 91–102.

Robin, A., Vansuyt, G., Hinsinger, P., Meyer, J.M., Briat, J.F., and Lemanceau, P. (2008) Iron dynamics in the rhizosphere: consequences for plant health and nutrition. *Adv Agron* **99:** 183–225.

Robinson, M.D., McCarthy, D.J., and Smyth, G.K. (2010) edgeR: a Bioconductor package for differential expression analysis of digital gene expression data. *Bioinformatics* **26:** 139–140.

Rodríguez, H., and Fraga, R. (1999) Phosphate solubilizing bacteria and their role in plant growth promotion. *Biotechnol Adv* **17:** 319–339.

Rosas, S.B., Andrés, J.A., Rovera, M., and Correa, N.S. (2006) Phosphate-solubilizing *Pseudomonas putida* can influence the rhizobia–legume symbiosis. *Soil Biol Biochem* **38:** 3502–3505.

Schink, B. (2002) Synergistic interactions in the microbial world. *Antonie Van Leeuwenhoek* **81:** 257–261.

Schirawski, J., and Perlin, M.H. (2018) Plant-microbe interaction 2017-the good, the bad and the diverse. *Int J Mol Sci* **19:** 1374.

Schloss, P.D., and Handelsman, J. (2005) Metagenomics for studying unculturable microorganisms: cutting the Gordian knot. *Genome Biol* **6:** 229.

Shariati, V., Malboobi, M.A., Tabrizi, Z., Tavakol, E., Owlia, P., and Safari, M. (2017) Comprehensive genomic analysis of a plant growth-promoting rhizobacterium *Pantoea agglomerans* strain P5. *Sci Rep* **7:** 1–12.

Sharma, S.B., Sayyed, R.Z., Trivedi, M.H., and Gobi, T.A. (2013) Phosphate solubilizing microbes: sustainable approach for managing phosphorus deficiency in agricultural soils. *SpringerPlus* **2:** 587.

Sigurbjörnsdóttir, M.A., Andresson, O.S., and Vilhelmsson, O. (2015) Analysis of the *Peltigera membranacea* metagenome indicates that lichen-associated bacteria are involved in phosphate solubilization. *Microbiology* **161:** 989–996.

Simons, M., Brand, I., Wijffelman, C.A., and Lugtenberg, B.J. (1996) Gnotobiotic system for studying rhizosphere colonization by plant growth-promoting *Pseudomonas* bacteria. *Mol Plant Microbe Interact* **9:** 600–607.

Smercina, D.N., Evans, S.E., Friesen, M.L., and Tiemann, L.K. (2019) To fix or not to fix: controls on free-living nitrogen fixation in the rhizosphere. *Appl Environ Microbiol* **85:** e02546–e2618.

Soni, A., Rokad, S., and Sharma, P. (2013) Screening of efficient halotolerant phosphate solubilizing bacteria and their effect on seed germination under saline conditions. *J Sci Innov Res* **2:** 932–937.

Souza, R.D., Ambrosini, A., and Passaglia, L.M. (2015) Plant growth-promoting bacteria as inoculants in agricultural soils. *Genet Mol Biol* **38:** 401–419.

Spaepen, S., Vanderleyden, J., and Remans, R. (2007) Indole-3-acetic acid in microbial and microorganism-plant signaling. *FEMS Microbiol Rev* **31:** 425–448.

Stewart, A.J., Chapman, W., Jenkins, G.I., Graham, I., Martin, T., and Crozier, A. (2001) The effect of nitrogen and phosphorus deficiency on flavonol accumulation in plant tissues. *Plant Cell Environ* **24:** 1189–1197.

Stewart, E.J. (2012) Growing unculturable bacteria. *J Bacteriol* **194:** 4151–4160.

Tanaka, T., Kawasaki, K., Daimon, S., Kitagawa, W., Yamamoto, K., Tamaki, H., *et al.* (2014) A hidden pitfall in the preparation of agar media undermines microorganism cultivability. *Appl Environ Microbiol* **80:** 7659–7666.

Toju, H., Peay, K.G., Yamamichi, M., Narisawa, K., Hiruma, K., Naito, K., *et al.* (2018) Core microbiomes for sustainable agroecosystems. *Nature Plants* **4:** 247–257.

Udaondo, Z., Duque, E., Daddaoua, A., Caselles, C., Roca, A., Pizarro-Tobias, P., and Ramos, J.L. (2020) Developing robust protein analysis profiles to identify bacterial acid phosphatases in genomes and metagenomic libraries. *Environ Microbiol* **22:** 3561–3571.

Ulrychová, M., and Sosnová, V. (1970) Effect of phosphorus deficiency on anthocyanin content in tomato plants. *Biol Plant* **12:** 231–235.

Venturi, V., and Keel, C. (2016) Signaling in the rhizosphere. *Trends Plant Sci* **21:** 187–198.

Walker, V., Bertrand, C., Bellvert, F., Moënne-Loccoz, Y., Bally, R., and Comte, G. (2011) Host plant secondary metabolite profiling shows a complex, strain-dependent response of maize to plant growth-promoting rhizobacteria of the genus *Azospirillum*. *New Phytol* **189:** 494–506.

Wang, C., Wang, H., Li, Y., Li, Q., Yan, W., Zhang, Y., *et al.* (2021) Plant growth-promoting rhizobacteria isolation from rhizosphere of submerged macrophytes and their growth-promoting effect on *Vallisneria natans* under high sediment organic matter load. *Microb Biotechnol* **14:** 726–736.

Wang, J., Pei, L., Jin, Z., Zhang, K., and Zhang, J. (2017) Overexpression of the protein phosphatase 2A regulatory

subunit a gene ZmPP2AA1 improves low phosphate tolerance by remodeling the root system architecture of maize. *PLoS One* **12:** e0176538.

Wang, Y.-C., Wang, N., Xu, H.-F., Jiang, S.-H., Fang, H.-C., Su, M.-y., *et al.* (2018a) Auxin regulates anthocyanin biosynthesis through the Aux/IAA–ARF signaling pathway in apple. *Horticult Res* **5:** 1–11.

Wang, Z.Q., Zhou, X., Dong, L., Guo, J., Chen, Y., Zhang, Y., *et al.* (2018b) iTRAQ-based analysis of the Arabidopsis proteome reveals insights into the potential mechanisms of anthocyanin accumulation regulation in response to phosphate deficiency. *J Proteomics* **184:** 39–53.

Wasaki, J., Sakaguchi, J., Yamamura, T., Ito, S., Shinano, T., Osaki, M., and Kandeler, E. (2018) P and N deficiency change the relative abundance and function of rhizosphere microorganisms during cluster root development of white lupin (*Lupinus albus* L.). *Soil Sci Plant Nutri* **64:** 686–696.

Wei, T., Simko, V., Levy, M., Xie, Y., Jin, Y., and Zemla, J. (2017) *R package Version 0.84*. URL https://cran.r-projec t.org/web/packages/corrplot/index.html.

Wright, R.J., Gibson, M.I., and Christie-Oleza, J.A. (2019) Understanding microbial community dynamics to improve optimal microbiome selection. *Microbiome* **7:** 85.

Yang, C.H., and Crowley, D.E. (2000) Rhizosphere microbial community structure in relation to root location and plant iron nutritional status. *Appl Environ Microbiol* **66:** 345–351.

Yang, Y., Wang, N., Guo, X., Zhang, Y., and Ye, B. (2017) Comparative analysis of bacterial community structure in the rhizosphere of maize by high-throughput pyrosequencing. *PLoS One* **12:** e0178425.

Yaryura, P., Cordon, G., León, M., Kerber, N., Pucheu, N., Rubio, G., *et al.* (2009) Effect of phosphorus deficiency on reflectance and chlorophyll fluorescence of cotyledons of oilseed rape (*Brassica napus* L.). *J Agron Crop Sci* **195:** 186–196.

Zhang, Y., Butelli, E., and Martin, C. (2014) Engineering anthocyanin biosynthesis in plants. *Curr Opin Plant Biol* **19:** 81–90.

Supporting information

Additional supporting information may be found online in the Supporting Information section at the end of the article.

Fig. S1. Overview of aboveground material from the *in planta* validation experiment after 21 days.

Fig. S2. Phenotypical appearance (A) and prevalence (B) of twisted and tightly folded, sticky whorls.

Fig. S3. Overview of different spectral images of the uninoculated negative control (plants supplied with insoluble P, FeP:AlP) and uninoculated positive control (plants supplied with soluble P, KH2PO4) as determined in the end-point measurement.

Fig. S4. Cumulative distribution of end-point mARI values per pixel of plants supplied with soluble P (KH$_2$PO$_4$, positive control) and supplied with insoluble P (FeP:AlP, negative control).

Fig. S5. Exponential relationship between the modified anthocyanin reflectance index (mARI) and plant P content in two independent experiments (exp.1: define calibration curve; exp.2: plants inoculated with bacterial suspensions).

Fig. S6. (A–C) Relative abundance of a selection of bacterial classes (resp. high, mid and low abundant classes) in the rhizosphere start suspension (*RSS*) and enriched suspensions (*V-B1-4*). Values represent the mean of six (*V-B1-4*) or three (*RSS*) biological replicates ± S.E. (D) Principal Components Analysis (PCA) biplot comprising bacterial classes (red arrows) and plant parameters (green arrows). Samples are coloured according to the corresponding treatment (*V-B*1 to 4). (E) Spearman correlation matrix between bacterial classes and important plant parameters.

Fig. S7. Relative abundance of bacterial orders in the rhizosphere start suspension (RSS) and enriched bacterial suspensions (V-Bn).

Fig. S8. Relative abundance of (a selection of) bacterial families in the rhizosphere start suspension (RSS) and enriched bacterial suspensions (V-Bn).

Table S1. Evaluation of plant's N:P and K:P ratio in maize plants throughout the enrichment experiment.

Table S2. Composition of different bacterial media used.

Table S3. GPS-coordinates and World Reference Base (WRB) classification of maize rhizosphere sampling sites

Table S4. Composition of modified Hoagland solution.